Journal of Prime Research in Mathematics

Optimal Control and Bifurcation Analysis of Cholera Model

Tulu Leta Tirfe[a], Legesse Lemecha Obsu[b], Eshetu Dadi Gurmu[b], Agbata Benedict Celestine[c], Shyamsunder[d,*]

[a]*Department of Mathematics, Bule Hora University, Bule Hora, Ethiopia.*
[b]*Department of Applied Mathematics, Adama Science and Technology University, Adama, Ethiopia.*
[c]*Department of Mathematics and Statistics, Faculty of Science, Confluence University of Science and Technology, Osara, Nigeria.*
[d]*Department of Mathematics, SRM University Delhi-NCR, Sonepat-131029, Haryana, India.*

Abstract

Cholera presents a significant public health challenge, especially in regions lacking access to clean water and proper sanitation. This study aims to develop an optimal control framework to effectively mitigate the dynamic spread of cholera and inform more efficient intervention strategies. Initially, we establish the well-posedness of the cholera transmission model, demonstrating the positivity and boundedness of solutions within a specified domain. Utilizing the next-generation matrix approach, we compute the basic reproduction number, a critical epidemiological threshold for disease dynamics. Upon obtaining a value below one, we employ the Jacobian matrix, Metzler matrix, and Lyapunov function analysis to verify the local and global stability of the cholera-free equilibrium. Sensitivity analysis highlights the significant impact of certain model parameters, such as the transmission rate and treatment efficacy, on cholera control. Leveraging the Pontryagin minimum principle, we formulate an optimal control problem to derive the most effective combination of prevention and treatment strategies. Numerical simulations illustrate that the optimal control approach, involving the simultaneous implementation of both interventions, surpasses standalone prevention or treatment measures in reducing the disease burden. This study underscores the importance of integrating prevention and treatment strategies for the effective mitigation of cholera outbreaks. The proposed optimal control framework provides a systematic approach for evaluating the impact of various interventions and informing public health policies. Future work will involve model extensions to incorporate spatial heterogeneity, fractional derivatives, and real-world data integration, enhancing the applicability and robustness of the control strategies.

Keywords: Cholera, Optimal Control, Stability, Global Stability, Local Stability
2010 Mathematics Subject Classification: Primary: 92D30, 49K15; Secondary: 34D23, 34D20, 93D05, 37N25.

*Corresponding author
Email addresses: tululeta2008@gmail.com (Tulu Leta Tirfe), legesse.lemecha@astu.edu.et (Legesse Lemecha Obsu), eshetudadi2020@gmail.com (Eshetu Dadi Gurmu), agbatacelestine92@gmail.com (Agbata Benedict Celestine), skumawatmath@gmail.com (Shyamsunder)

1. Introduction

Infectious diseases are pathological conditions caused by various microorganisms, including bacteria, viruses, parasites, and fungi. These illnesses can propagate through direct or indirect means, posing a significant hazard to global public health, often resulting in considerable morbidity and mortality during outbreaks [1]. Implementing effective control measures is imperative for curtailing the dissemination of these diseases and minimizing their consequences. Inadequate hygiene practices and close proximity between infected and susceptible individuals are primary factors contributing to the transmission of diverse infectious diseases [1, 2, 3].

Cholera stands out as a prominent infectious disease characterized by severe acute watery diarrhea induced by the bacterium Vibrio cholerae. Typical symptoms include intense diarrhea, vomiting, and dehydration, which can prove fatal if left untreated [4]. Cholera disproportionately impacts populations in developing regions with limited access to sanitary water and proper hygiene facilities. The disease persists in these areas due to deficient infrastructure and public health resources [1]. Transmission occurs through both direct (person-to-person) and indirect (contaminated water sources) pathways, resulting in rapid dissemination and elevated mortality rates in the absence of adequate management [1, 3].

Mathematical modeling has become a valuable tool for understanding and managing the dynamics of infectious diseases, including cholera [5, 6]. Mathematical epidemiology aids in describing disease behaviour, influencing factors, and forecasting its spread. Several studies have proposed deterministic models to explore various aspects of cholera transmission, such as endemicity, environmental influences, and stochastic elements. For example, Hartley et al. [7] highlighted the importance of incorporating environmental reservoirs in cholera models to better understand its persistence and spread. Tien and Earn (2010) examined the role of seasonality in cholera transmission and emphasized the need for models that account for environmental variability [8].

Despite these advancements, a comprehensive modeling framework is still needed to integrate key interventions such as vaccination and treatment to inform more effective control strategies. Azman et al. [9] demonstrated the potential impact of oral cholera vaccines in reducing disease incidence and highlighted the importance of vaccination campaigns in endemic regions. Other studies, such as those by Chang et al. [10], have explored the cost-effectiveness of different control measures, providing valuable insights for public health policy. Ali et al. [11] presented updated global burden data, highlighting ongoing challenges in endemic countries. Codeco (2001) explored the dynamics of cholera transmission, emphasizing the role of aquatic reservoirs in sustaining outbreaks. Andrews and Basu (2011) offered an epidemic model that elucidates transmission dynamics and control strategies, particularly relevant in crisis contexts such as Haiti [12]. Bhattacharya et al. [13] discussed public health interventions, emphasizing the urgency of coordinated efforts during outbreaks.

Studies by Azman et al. [14] have focused on integrating genomic data with epidemiological models to track the transmission dynamics of cholera strains. This approach has provided insights into strain evolution, transmission pathways, and potential impacts on vaccine effectiveness, informing more targeted vaccination strategies and outbreak response efforts. In parallel, research by Finger et al. [15] has emphasized the role of climate variability and environmental factors in cholera dynamics. Their work highlights how climate change influences waterborne diseases like cholera through altered hydrological patterns and water quality, underscoring the need for adaptive strategies that account for environmental resilience and health equity. Furthermore, recent studies by Azman et al. [16] have evaluated the impact of integrated control strategies combining vaccination with improved water and sanitation infrastructure. Their findings demonstrate synergistic benefits in reducing cholera incidence and transmission rates, advocating for comprehensive, multi-sectoral approaches to cholera prevention and control.

Tilahun et al. [3] developed a cholera model featuring compartments representing susceptible, infectious, treated, and recovered individuals. This model simulates cholera transmission dynamics, where susceptible individuals can become infected upon contact with infectious individuals, recover with treatment, or acquire immunity after recovery. Key parameters include transmission rates, recovery rates, and environmental

factors affecting disease spread. Their model also explores interventions such as vaccination and treatment strategies to assess their impact on controlling cholera outbreaks.

In summary, infectious diseases like cholera pose significant public health challenges. Understanding their transmission dynamics and developing effective control strategies through mathematical modeling and empirical research are crucial for mitigating their impact, particularly in vulnerable populations. The present study introduces a novel cholera model, SVITR (Susceptible-Vaccinated-Infectious-Treatment-Recovered), which extends the framework developed by Tilahun et al. by incorporating a vaccination compartment, bifurcation analysis, and exploring the impact of optimal control strategies on disease dynamics. This model aims to capture both the direct transmission pathway of cholera and the effects of vaccination as a preventive measure.

The structure of the paper is organized as follows: Section 2 outlines the formulation of the SVITR cholera model within a deterministic framework, detailing how it integrates vaccination dynamics with predictable disease compartments. Section 3 conducts qualitative and sensitivity analyses to understand the model's behaviour and identify critical parameters influencing cholera dynamics. Section 4 focuses on the development of an optimal control problem, using mathematical techniques such as the Pontryagin minimum principle to determine the most effective combination of prevention and treatment interventions. Section 5 presents numerical simulations and results that demonstrate the efficacy of these optimal control strategies in reducing the disease burden. Finally, Section 6 discusses the implications of the findings and draws conclusions regarding the effectiveness of integrating vaccination with other control measures in cholera management. This structured approach aims to provide comprehensive insights into enhancing cholera control strategies through mathematical modeling and optimal intervention planning.

2. Cholera Model Description and Formulation

To capture the complex dynamics of cholera transmission and the impact of intervention strategies, we developed a deterministic epidemiological model that categorizes the population into five distinct compartments based on their disease status: Susceptible (S), Vaccinated (V), Infectious (I), Treated (T), and Recovered (R).

The model assumes that a fraction (α) of the total population (Π) has been vaccinated against cholera before the outbreak, while the remaining $(1-\alpha)\Pi$ individuals are initially susceptible. Susceptible individuals can become infected upon contact with infectious individuals, at a rate determined by the transmission coefficient (β) and the force of infection $(\lambda = \frac{\beta I}{N})$. The vaccine is assumed to provide partial immunity, reducing the infection rate among vaccinated individuals to $(1-p)\eta$, where $p \in (0,1)$ represents the vaccine efficacy, and η is the per capita rate of becoming infectious. Vaccinated individuals can lose their immunity over time and revert to the susceptible class at a rate of $p\eta$.

Infected individuals transition to the treatment class at a rate (ω) and may either recover from the disease at a rate (γ) or succumb to the infection at a rate (ξ). Those in the treatment class undergo medical treatment, with the potential for treatment failure leading to mortality at the same rate (ξ). Recovered individuals may gradually lose their immunity and return to the susceptible class at a rate (δ). All individuals in the population are subject to natural mortality at a rate (μ). The model parameters are constrained to be non-negative.

The flow diagram in Fig. 1 illustrates the relationships and transitions between the different compartments of the SVITR cholera model. The mathematical formulation of the model is as follows: From the assumptions with the description and the schematic diagram we obtained the following model equations;
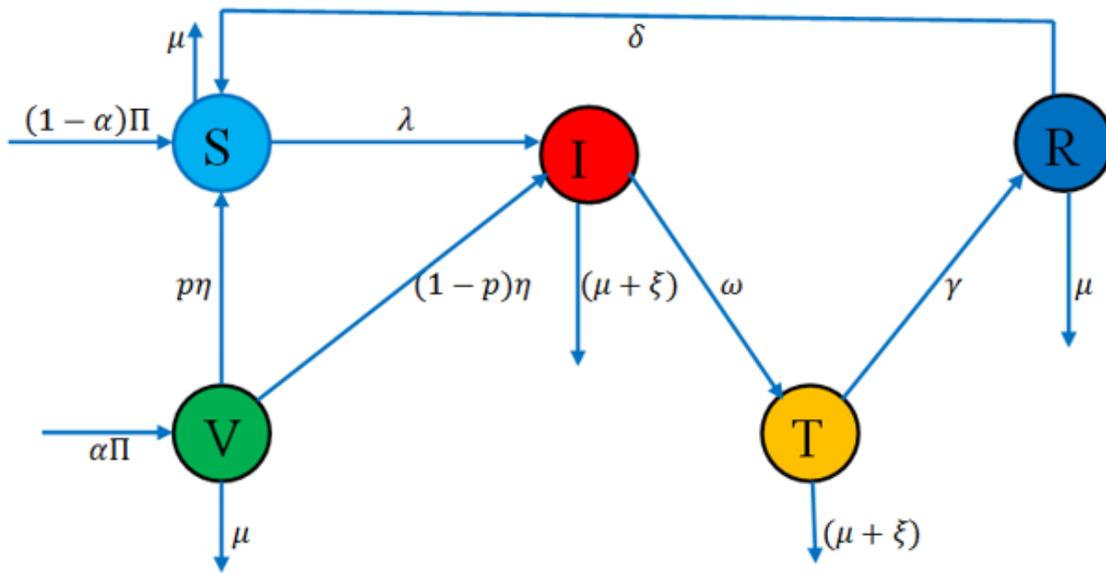
Figure 1: Schematic diagram of Cholera model

$$
\begin{cases}
\frac{dS}{dt} = (1 - \alpha)\,\Pi - (\lambda + \mu)\,S + p\eta V + \delta R, \\
\frac{dV}{dt} = \alpha\Pi - (\eta + \mu)\,V, \\
\frac{dI}{dt} = \lambda S + (1 - p)\,\eta V - (\omega + \mu + \xi)\,I, \\
\frac{dT}{dt} = \omega I - (\gamma + \mu + \xi)\,T, \\
\frac{dR}{dt} = \gamma T - (\delta + \mu)\,R,
\end{cases}
\tag{2.1}
$$

where,

$\lambda = \frac{\beta I}{N}$ with initial condition $S(0) > 0, V(0) > 0, I(0) \geq 0, T(0) \geq 0$, and $R(0) \geq 0$.

The SVITR model extends the previous work by Tilahun et al [3] by explicitly incorporating a vaccination compartment and exploring the direct transmission pathway, which is crucial for understanding the impact of immunization strategies on cholera control. The model formulation and analysis presented in the following sections aim to provide insights into the disease dynamics and identify the optimal combination of prevention and treatment interventions to mitigate cholera outbreaks effectively.

3. Basic Properties of Cholera Model

3.1. Existence and Uniqueness of the Solutions

Lemma 3.1. *(Existence and Uniqueness). In model (2.1) if the initial conditions $S(0) \geq 0, V(0) \geq 0, I(0) \geq 0, T(0) \geq 0$, $R(0) \geq 0$, then for all $t > 0$ the solutions $S(t), V(t), I(t), T(t), R(t)$ exists in $\mathbb{R}_+^5$.*

Proof. Model (2.1) can be expressed in the form $\dot{x} = f(x)$, where

$$\dot{x} = [S, V, I, T, R]^T = \begin{bmatrix} S(t) \\ V(t) \\ I(t) \\ T(t) \\ R(t) \end{bmatrix}.$$

$$f(x) = \begin{bmatrix} (1-\alpha)\Pi - (\lambda+\mu)S + p\eta V + \delta R \\ \alpha\Pi - (\eta+\mu)V \\ \lambda S + (1-p)\eta V - (\omega+\mu+\xi)I \\ \omega I - (\gamma+\mu+\xi)T \\ \gamma T - (\delta+\mu)R \end{bmatrix} = \begin{bmatrix} f_1 \\ f_2 \\ f_3 \\ f_4 \\ f_5 \end{bmatrix}.$$

Moreover, let us compute the following partial derivatives,

$$\begin{cases} \frac{\partial f_1}{\partial S} = -(\lambda+\mu), & \frac{\partial f_1}{\partial V} = (p\eta), & \frac{\partial f_1}{\partial I} = 0, & \frac{\partial f_1}{\partial T} = 0, & \frac{\partial f_1}{\partial R} = \delta, \\ \frac{\partial f_2}{\partial S} = 0, & \frac{\partial f_2}{\partial V} = -(\eta+\mu), & \frac{\partial f_2}{\partial I} = 0, & \frac{\partial f_2}{\partial T} = 0, & \frac{\partial f_2}{\partial R} = 0, \\ \frac{\partial f_3}{\partial S} = \lambda, & \frac{\partial f_3}{\partial V} = (1-p)\eta, & \frac{\partial f_3}{\partial I} = -(\omega+\mu+\xi), & \frac{\partial f_3}{\partial T} = 0, & \frac{\partial f_3}{\partial R} = 0, \\ \frac{\partial f_4}{\partial S} = 0, & \frac{\partial f_4}{\partial V} = 0, & \frac{\partial f_4}{\partial I} = \omega, & \frac{\partial f_2}{\partial T} = -(\gamma+\mu+\xi), & \frac{\partial f_4}{\partial R} = 0, \\ \frac{\partial f_5}{\partial S} = 0, & \frac{\partial f_5}{\partial V} = 0, & \frac{\partial f_5}{\partial I} = 0, & \frac{\partial f_5}{\partial T} = \gamma, & \frac{\partial f_5}{\partial R} = -(\delta+\mu). \end{cases}$$

Thus, f satisfies the Lipschitz condition and has continuous first partial derivatives with respect to state variable in $\mathbb{R}_+^5$ locally. Hence, there exists a unique solution of the model by Picard-Lindelof existence and uniqueness theorem [36]. □

3.2. Invariant Region

Theorem 3.2. *If the initial conditions of the model (2.1) are in,*

$$\Gamma = \left\{ (S, V, I, T, R) \in \mathbb{R}_+^5 : 0 \le N(t) \le \frac{\Pi}{\mu} \right\},$$

then all future solutions of the system equation of the model enter and remain in Γ.

Proof. A region in which solutions of the model system are uniformly bounded is the proper subset $\Gamma \subset \mathbb{R}_+^5$. The total population at a time t is given by $N(t) = S(t) + V(t) + I(t) + T(t) + R(t)$. After differentiating both sides of $N(t)$,

$$\frac{dN(t)}{dt} = \frac{dS(t)}{dt} + \frac{dV(t)}{dt} + \frac{dI(t)}{dt} + \frac{dT(t)}{dt} + \frac{dR(t)}{dt}. \tag{3.1}$$

Substituting

$$\frac{dS(t)}{dt}, \frac{dV(t)}{dt}, \frac{dI(t)}{dt}, \frac{dT(t)}{dt}, \text{ and } \frac{dR(t)}{dt}$$

from equation (2.1) into equation (3.1), we obtain

$$\frac{dN(t)}{dt} = \Pi - \mu N(t) - \xi I - \xi T. \tag{3.2}$$

In the absence of mortality due to cholera disease ($\xi = 0$), then equation (3.2) becomes

$$\frac{dN(t)}{dt} \le \Pi - \mu N(t). \tag{3.3}$$

Rearranging and integrating both sides of (3.3) and considering initial condition, we get

$$N(t) \leq \frac{\Pi}{\mu} - \left[\frac{\Pi - \mu N(t)}{\mu}\right] e^{-\mu t}. \tag{3.4}$$

Further, it can be observed that the total population size, $N(t)$, converges to the value $\frac{\Pi}{\mu}$ as time approaches infinity. Specifically, we can show that $N(t) \longrightarrow \frac{\Pi}{\mu}$ as $t \longrightarrow \infty$.

This means that the total population size, $N(t)$, starts from the initial value $N(0)$ and approaches the bounded value of $\frac{\Pi}{\mu}$ as time grows. In other words, the total population size is bounded between 0 and $\frac{\Pi}{\mu}$, with the upper bound representing the carrying capacity of the population.

Mathematically, we can express this as: $0 \leq N(t) \leq \frac{\Pi}{\mu}$. This implies that the feasible solution set of the system of differential equations governing the model dynamics enters and remains within the region defined by this inequality. In other words, the total population size is confined to the interval $[0, \frac{\Pi}{\mu}]$, ensuring the boundedness and non-negativity of the model solutions.

This property of the total population size is crucial for the well-posedness and stability analysis of the cholera model, as it guarantees that the solutions remain biologically meaningful and within realistic bounds. □

3.3. Positivity of Solutions

The solution of the system remains positive at any point in time t, if the initial values of all the variables are positive.

Lemma 3.3. *The solution of the model (2.1) with a non-negative initial condition remains non-negative for all $t \geq 0$.*

Proof. Positivity is verified separately for each of the model variable $S(t), V(t), I(t), T(t)$, and $R(t)$.
Positivity of $S(t)$: From model equation (2.1) we have,

$$\frac{dS}{dt} = (1 - \alpha)\Pi - (\lambda + \mu)S + p\eta V + \delta R,$$

$$\frac{dS}{dt} > -(\lambda + \mu)S,$$

$$\frac{dS}{S} > -(\lambda + \mu)dt.$$

After solving equation by using the separation of variables and applying the initial conditions, we get

$$S(t) > S_0 e^{-(\lambda+\mu)t}, \; S_0 = e^{c_3} \text{ and } e^{-(\lambda+\mu)t} > 0, \text{ for all } t \geq 0.$$

Hence, $S(t) > S_0 e^{-(\lambda+\mu)t} > 0$.

Similarly using the other equations of system (2.1), positivity of solutions can be established as follows:
$V(t) > V_0 e^{-(\eta+\mu)t} > 0$,
$I(t) \geq I_0 e^{-(\omega+\mu+\xi)t} \geq 0$,
$T(t) \geq T_0 e^{-(\gamma+\mu+\xi)t} \geq 0$,
$R(t) \geq R_0 e^{-(\delta+\mu)t} \geq 0$.

Hence, all the solutions of the model equation (2.1) are positive for all $t \geq 0$.

Therefore, the model variables $S(t), V(t), I(t), T(t)$, and $R(t)$ representing population sizes of various types of cells are positive quantities and will remain in $\mathbb{R}_+^5$ for all t. □

3.4. Equilibrium Analysis

3.5. Cholera Free Equilibrium

To determine the cholera-free equilibrium point, we set the right-hand side of the model equations (2.1) to zero, which corresponds to the steady-state condition where there are no infectious individuals in the population.

$$
\begin{cases}
(1-\alpha)\Pi - (\lambda + \mu)S + p\eta V + \delta R = 0, \\
\alpha\Pi - (\eta + \mu)V = 0, \\
\lambda S + (1-p)\eta V - (\omega + \mu + \xi)I = 0, \\
\omega I - (\gamma + \mu + \xi)T = 0, \\
\gamma T - (\delta + \mu)R = 0.
\end{cases}
\tag{3.5}
$$

Then the system of equations (3.5) is simplified, gives

$$
\begin{cases}
(1-\alpha)\Pi - (\lambda + \mu)S + p\eta V + \delta R = 0, \\
\alpha\Pi - (\eta + \mu)V = 0.
\end{cases}
$$

By solving the above equation we get

$$
S_0 = \frac{\Pi[((\eta+\mu)+\alpha(\eta p - \eta - \mu))]}{\mu(\eta+\mu)} \text{ and } V_0 = \frac{\alpha\Pi}{\eta+\mu}.
$$

Therefore, our cholera-free equilibrium point is

$$
E_0 = \left(\frac{\Pi[(\eta+\mu)+\alpha(\eta p - \eta - \mu)]}{\mu(\eta+\mu)}, \frac{\alpha\Pi}{\eta+\mu}, 0, 0, 0 \right),
$$

if $\eta p > (\eta + \mu)$ holds. Which means disease free equilibrium is positive.

3.6. Basic Reproduction Number (R_0)

The basic reproductive number, denoted by R_0, quantifies the average number of secondary infections stemming from a single infected individual. This metric serves as a pivotal threshold for system stability. Conceptually, it corresponds to the spectral radius of the next-generation matrix. To compute it, the model system (2.1) is restructured, beginning with the components representing newly infective classes [13].

$$
\begin{cases}
\frac{dI}{dt} = \lambda S + (1-P)\eta V - (\omega + \mu + \xi)I, \\
\frac{dT}{dt} = \omega I - (\gamma + \mu + \xi)T.
\end{cases}
\tag{3.6}
$$

Let $Z = [I, T]^T$ denote a vector of infectious variables, then

$$
\frac{dZ}{dt}|E_0 = F(Z) - V(Z) = \begin{bmatrix} \frac{\beta S}{N} + (1-p)\eta V \\ 0 \end{bmatrix} - \begin{bmatrix} (\omega + \mu + \xi)I \\ -\omega I + (\gamma + \mu + \xi)T \end{bmatrix}.
$$

with the next-generation matrices

$$
F = \frac{\partial F(Z)}{\partial Z}|_{E_0} = \begin{bmatrix} \frac{\beta S_0}{S_0 + V_0} & 0 \\ 0 & 0 \end{bmatrix}, V = \frac{\partial V(Z)}{\partial Z}|_{E_0} = \begin{bmatrix} \omega + \mu + \xi & 0 \\ -\omega & \gamma + \mu + \xi \end{bmatrix}.
$$

Then, evaluating F and V at a disease-free equilibrium point

$$
E_0 = \left(\frac{\Pi[(\eta+\mu)+\alpha(\eta p - \eta - \mu)]}{\mu(\eta+\mu)}, \frac{\alpha\Pi}{\eta+\mu}, 0, 0, 0 \right)
$$

which leads to

$$
FV^{-1} = \begin{bmatrix} \frac{\beta S_0}{(S_0 + V_0)(\omega+\mu+\xi)} & \frac{\beta S_0 \omega}{(S_0 + V_0)(\omega+\mu+\xi)(\gamma+\mu+\xi)} \\ 0 & 0 \end{bmatrix}.
$$

The eigenvalue of FV^{-1} can be obtained by

$$\begin{vmatrix} \frac{\beta S_0}{(S_0+V_0)(\omega+\mu+\xi)} - \lambda & \frac{\beta S_0 \omega}{(S_0+V_0)(\omega+\mu+\xi)(\gamma+\mu+\xi)} \\ 0 & 0 - \lambda \end{vmatrix} = 0.$$

Here, according to the principle of the next-generation matrix, the basic reproduction number is determined as the largest eigenvalue,

$$R_0 = \frac{\beta S_0}{(S_0 + V_0)(\omega + \mu + \xi)}.$$

After we substitute S_0 and V_0

$$R_0 = \frac{\beta \left[\eta + \mu + \alpha(\eta p - \eta - \mu) \right]}{\left([\eta + \mu + \alpha(\eta p - \eta - \mu)] + \alpha\mu \right)(\omega + \mu + \xi)}.$$

3.7. Local Stability of Cholera Free Equilibrium

Theorem 3.4. *Disease-free equilibrium E_0 of system of equations given in (2.1) is locally asymptotically stable if $R_0 < 1$ and unstable if $R_0 > 1$.*

Proof. Now, the Jacobian matrix of the model equations given in (2.1) at the cholera-free equilibrium E_0 gives the form :

$$\begin{cases} \frac{dS}{dt} = (1-\alpha)\Pi - (\lambda + \mu)S + p\eta V + \delta R = f_1, \\ \frac{dV}{dt} = \alpha\Pi - (\eta + \mu)V = f_2, \\ \frac{dI}{dt} = \lambda S + (1-p)\eta V - (\omega + \mu + \xi)I = f_3, \\ \frac{dT}{dt} = \omega I - (\gamma + \mu + \xi)T = f_4, \\ \frac{dR}{dt} = \gamma T - (\delta + \mu)R = f_5. \end{cases} \qquad (3.7)$$

Then the Jacobian matrix at E_o becomes:

$$J = \begin{bmatrix} -\mu & p\eta & -\frac{\beta S_0}{S_0+V_0} & 0 & \delta \\ 0 & -(\eta + \mu) & 0 & 0 & 0 \\ 0 & (1-p)\eta & \frac{\beta S_0}{S_0+V_0} - (\omega + \mu + \xi) & 0 & 0 \\ 0 & 0 & \omega & -(\gamma + \mu + \xi) & 0 \\ 0 & 0 & 0 & \gamma & -(\delta + \mu) \end{bmatrix}$$

Then the Jacobian matrix evaluated at E_0 becomes

$$J(E_0) = \begin{bmatrix} -\mu & p\eta & \frac{\beta(\eta\mu\alpha(\eta p-\eta-\mu))}{\eta\mu\alpha(\eta p-\eta-\mu)+\mu\alpha} & 0 & \delta \\ 0 & -(\eta + \mu) & 0 & 0 & 0 \\ 0 & (1-p)\eta & \frac{\beta S_0}{S_0+V_0} - (\omega + \mu + \xi) & 0 & 0 \\ 0 & 0 & \omega & -(\gamma + \mu + \xi) & 0 \\ 0 & 0 & 0 & \gamma & -(\delta + \mu) \end{bmatrix}$$

Computing the eigen polynomial we obtain,

$$J(E_0) = \begin{vmatrix} -\mu - \lambda & p\eta & -b & 0 & \delta \\ 0 & -(\eta + \mu) - \lambda & 0 & 0 & 0 \\ 0 & (1-p)\eta & b - (\omega + \mu + \xi) - \lambda & 0 & 0 \\ 0 & 0 & \omega & -(\gamma + \mu + \xi) - \lambda & 0 \\ 0 & 0 & 0 & \gamma & -(\delta + \mu) - \lambda \end{vmatrix} = 0$$

where, $b = \frac{\beta(\eta+\mu+\alpha(\eta p-\eta-\mu))}{(\eta+\mu+\alpha(\eta p-\eta-\mu)+\mu\alpha)}$.

$$(-\mu - \lambda)(-(\eta + \mu) - \lambda)(b - (\omega + \mu + \xi) - \lambda)(-(\delta + \mu + \xi) - \lambda)(-(\delta + \mu) - \lambda) = 0. \qquad (3.8)$$

Solving this one can easily obtain that,

$$\lambda_1 = -\mu, \lambda_2 = -(\eta + \mu), \lambda_3 = b - (\omega + \mu + \xi), \lambda_4 = -(\delta + \mu + \xi) \text{ and } \lambda_5 = -(\delta + \mu).$$

Since

$$\lambda_1 < 0, \ \lambda_2 < 0, \ \lambda_4 < 0, \ \lambda_5 < 0,$$

know the sign of all eigenvalues are negative. If $\lambda_3 = b - (\omega + \mu + \xi) < 0$. These means $R_0 < 1$.

Therefore, our disease-free equilibrium point is locally asymptotically stable if and only if $R_0 < 1$. $\qquad \square$

3.8. Global Stability of Cholera Free Equilibrium

The global stability of disease free equilibrium was implemented by Castillo-Chavez and Song technique [12]. The model equation (2.1) can be re-written as

$$\begin{cases} \frac{dX}{dt} = F(X, Z), \\ \frac{dZ}{dt} = G(X, Z), \end{cases}$$

where, X stands for the uninfected population, that is $X = (S, V, R)^T$ and Z also stands for the infected population, that is $Z = (I, T)^T$. The disease free equilibrium point of the model is denoted by $U = (X^*, 0)$. The point $U = (X^*, 0)$ to be globally asymptotically stable equilibrium for the model provided that $R_0 < 1$ and the following conditions must be met: According to [15], to guarantee global asymptotic stability, we verify the following conditions H_1 and H_2 to be satisfied:

i. H_1: for $\frac{dX}{dt} = F(X, 0), X^*$ is the globally asymptotically stable equilibrium.
ii. H_2: $G(X, Z) = AZ - \hat{G}(X, Z), \hat{G}(X, Z) \geq 0$ for $(X, Z) \in \Gamma$.

Where $A = D_Z G(U, 0)$ a Metzler's matrix is i.e. the off diagonal elements of A are non-negative and G is the region where the model makes biologically sense. If the model (2.1) met the above two criteria then the following theorem holds.

Theorem 3.5. *The point $U = (X^*, 0)$ is globally asymptotically stable equilibrium provided that $R_0 < 1$ and the condition (H_1) and (H_2) are satisfied.*

Proof. From system (2.1) we can get $F(X, Z)$ and $G(X, Z)$;

$$F(X, Z) = \begin{bmatrix} (1 - \alpha)\Pi - (\lambda + \mu)S + p\eta V + \delta R \\ \alpha\Pi - (\eta + \mu)V \\ \gamma T - (\delta + \mu)R \end{bmatrix}$$

and

$$G(X, Z) = \begin{bmatrix} \lambda S + (1 - p)\eta V - (\omega + \mu + \xi)I \\ \omega I - (\gamma + \mu + \xi)T \end{bmatrix}.$$

Consider the reduced system:

$$\frac{dX}{dt}\Big|_{Z=0} = \begin{bmatrix} (1 - \alpha)\Pi - \mu S + p\eta V + \delta R \\ \alpha\Pi - (\eta + \mu)V \\ \gamma T - (\delta + \mu)R \end{bmatrix}. \qquad (3.9)$$

From (2.1) it is obvious that

$$X^* = \left(\frac{\Pi[(\eta+\mu)+\alpha(\eta p-\eta-\mu)]}{\mu(\eta+\mu)}, \frac{\alpha\Pi}{\eta+\mu}, 0 \right).$$

is the global asymptotic point. This can be verified from the solution, namely,

$$S = \left(\frac{\Pi[(\eta+\mu)+\alpha(\eta p-\eta-\mu)]}{\mu(\eta+\mu)}\right) + [S(0) - \left(\frac{\Pi[(\eta+\mu)+\alpha(\eta p-\eta-\mu)]}{\mu(\eta+\mu)}\right)]e^{-\mu t}.$$

$$V = \left(\frac{\alpha\Pi}{\eta+\mu}\right) + [V(0) - \left(\frac{\alpha\Pi}{\eta+\mu}\right)]e^{-\mu t}.$$

As $t \longrightarrow \infty$, the solution $S = \left(\frac{\Pi[(\eta+\mu)+\alpha(\eta p-\eta-\mu)]}{\mu(\eta+\mu)}\right)$ and $V = \left(\frac{\alpha\Pi}{\eta+\mu}\right)$ implying the global convergence of (2.1) in Γ.

From the equation for infected compartments in the model we have

$$A = \begin{bmatrix} \frac{\beta(\eta\mu\alpha(\eta p-\eta-\mu))}{\eta\mu\alpha(\eta p-\eta-\mu)+\mu\alpha} - h_1 & 0 \\ \omega & -h_2 \end{bmatrix}.$$

Since A is Metzler matrix, i.e, all off-diagonal elements are nonnegative, then, $G(X, Z)$ can be written as
$G(X, Z) = AZ - \hat{G}(X, Z)$, where

$$\hat{G}(X, Z) = \begin{bmatrix} \hat{G}_1(X, Z) \\ \hat{G}_2(X, Z) \\ \hat{G}_3(X, Z) \end{bmatrix} = \begin{bmatrix} 0 \\ 0 \\ 0 \end{bmatrix}.$$

It follows that

$$\hat{G}_1(X, Z) = \hat{G}_2(X, Z) = \hat{G}_3(X, Z) = 0.$$

Thus conditions H_1 and H_2 are satisfied and we conclude that E_0 is globally asymptotically stable for $R_0 < 1$. □

3.9. Cholera Persistence Equilibrium

The equilibrium of the model (2.1) is denoted by $E_1^* = (S^*, V^*, I^*, T^*, R^*)$ and defined as a steady-state solutions for the model (2.1). This can occur when there is a persistence of the disease. It can be obtained by equating the system of equation (2.1) equal to zero:

$$\begin{cases} (1 - \alpha)\Pi - (\lambda + \mu)S + p\eta V + \delta R = 0, \\ \alpha\Pi - (\eta + \mu)V = 0, \\ \lambda S + (1 - p)\eta V - (\omega + \mu + \xi)I = 0, \\ \omega I - (\gamma + \mu + \xi)T = 0, \\ \gamma T - (\delta + \mu)R = 0. \end{cases} \tag{3.10}$$

From the second equation of system (3.10), we get

$$\alpha\Pi - (\eta + \mu)V = 0.$$

Then, solving for V^*, we have

$$V^* = \frac{\alpha\Pi}{\eta + \mu}. \tag{3.11}$$

From the fourth equation in (3.10), we solve for I^*:

$$I^* = \frac{(\gamma + \mu + \xi)T^*}{\omega}. \tag{3.12}$$

Now, solving for S^* by substituting equation (3.11) and (3.12) into the third equation of (3.10), we obtain

$$S^* = \frac{(\omega + \mu + \xi)(\gamma + \mu + \xi)}{\lambda \omega}T^* - \frac{(1 - p)\alpha \eta \Pi}{\eta + \mu}. \tag{3.13}$$

Solving simultaneously the fourth and fifth equation of (3.10), we get

$$\begin{cases} \omega I - (\gamma + \mu + \xi)T = 0, \\ \gamma T - (\delta + \mu)R = 0. \end{cases} \tag{3.14}$$

$$R^* = \frac{\gamma \omega I^*}{(\delta + \mu)(\gamma + \mu + \xi)}. \tag{3.15}$$

Then substituting equation (3.15) into the second equation of (3.14), we have

$$T^* = \frac{\omega I^*}{(\gamma + \mu + \xi)}. \tag{3.16}$$

Therefore, endemic equilibrium point of the model is

$$E_1^*(S^*, V^*, I^*, T^*, R^*) = \left(\frac{(\omega+\mu+\xi)\omega I^*}{\lambda\omega} - \frac{(1-p)\alpha\eta\Pi}{\eta+\mu}, \frac{\alpha\Pi}{\eta+\mu}, I^*, \frac{\omega I^*}{(\gamma+\mu+\xi)}, \frac{\gamma\omega I^*}{(\delta+\mu)(\gamma+\mu+\xi)} \right).$$

3.10. Global Stability of Cholera Persistence Equilibrium Point

Theorem 3.6. *If $R_0 > 1$, then the EEP given by $E_1 = (S^*, V^*, I^*, T^*, R^*)$; is globally asymptotically stable in the region Γ.*

Proof. Suppose the basic reproductive number $R_0 > 1$ so that the EEP exists.
    Consider a Lyapunov function candidate L defined by,

$$L(S, V, I, T, R) =$$
$$(S - S^* - \ln\frac{S}{S^*}) + (V - V^* - V^*\ln\frac{V}{V^*}) + (I - I^* - I^*\ln\frac{I}{I^*}) + (T - T^* - T^*\ln\frac{T}{T^*}) + (R - R^* - R^*\ln\frac{R}{R^*}).$$

Differentiating L in the direction of (2.1) leads to,

$$\frac{dL}{dt} = (\frac{S-S^*}{S})\dot{S} + (\frac{V-V^*}{V})\dot{V} + (\frac{I-I^*}{I})\dot{I} + (\frac{T-T^*}{T})\dot{T} + (\frac{R-R^*}{R})\dot{R}.$$

Replacing $\dot{S}, \dot{V}, \dot{I}, \dot{T}, \dot{R}$ by their respective expression from model (2.1) we get,

$$\frac{dL}{dt} = (\frac{S-S^*}{S})((1-\alpha)\Pi - (\lambda + \mu)S + p\eta V + \delta R) + (\frac{V-V^*}{V})(\alpha\Pi - (\eta + \mu)V) + (\frac{I-I^*}{I})(\lambda S + (1-p)\eta V$$
$$\text{-}(\omega + \mu + \xi)I) + (\frac{T-T^*}{T})(\omega I - (\gamma + \mu + \xi)T) + (\frac{R-R^*}{R})(\gamma T - (\delta + \mu)R).$$

$$(\frac{S-S^*}{S})(\Pi + \alpha V + \delta R - (\eta + \frac{\beta I}{N} + \mu)(S - S^*) - (\eta + \frac{\beta I}{N} + \mu)S^*) + (\frac{V-V^*}{V}(\eta S - (1-p)\frac{\beta I}{N}(V - V^*))$$
$$\text{-}(\alpha + \mu)(V - V^*) - (1-p)\frac{\beta I}{N}V^* - (\alpha + \mu)V^*) + (\frac{(I-I^*)^2}{I})(\frac{\beta}{N}S(I - I^*) + (1-p)\frac{\beta}{N}V(I - I^*) - (\omega + \mu +$$
$$\xi)(I - I^*)) - (\frac{(1-\varphi)}{N}\beta V I^*) + \frac{\beta S I^*}{N} - (\omega + \mu + \xi)I^*) + (\frac{(T-T^*)^2}{T})(\omega I - (\gamma + \mu + \xi)T)$$
$$+(\frac{R-R^*}{R}(\gamma T - (\delta + \mu)R - (\delta + \mu)(R - R^*) - (\delta + \mu)R^*).$$

$$-\frac{(S-S^*)^2}{S}(\eta + \frac{\beta I}{N} + \mu) + \Pi + \alpha V + \delta R - \frac{S^*}{S}(\Pi + \alpha V + \delta R) - (\eta + \frac{\beta I}{N} + \mu)S^* + \frac{(S^*)^2}{S}(\eta + \frac{\beta I}{N} + \mu)$$
$$+\frac{-(V-V^*)^2}{V}(\frac{(1-p)\beta I}{N} + (\alpha + \mu)) + \eta S - \frac{V^*}{V}\eta S - (\frac{(1-p)\beta I V^*}{N}) + \frac{(1-p)\beta I(V^*)^2}{NV} - (\alpha + \mu)V^* + \frac{(\alpha+\mu)(V^*)^2}{V}$$
$$\text{-}\frac{(I-I^*)^2}{I}(-(1-p)\frac{\beta V}{N} + (\omega + \mu + \xi) - \frac{\beta S}{N}) - \frac{\beta S}{N}I^* - \frac{\beta S I^{*2}}{NI} - \frac{(1-p)\beta V I^*}{N} + \frac{(1-\varphi)\beta V(I^*)^2}{NI} - (\omega + \mu + \xi)I^*$$
$$+(\omega + \mu + \xi)\frac{(I^*)^2}{I} - \frac{(T-T^*)^2}{T}(\gamma + \mu) + \omega I - \frac{T^*}{T}\omega I - (\gamma + \mu)T^* + (\gamma + \mu)\frac{(T^*)^2}{T} - \frac{(R-R^*)^2}{R}(\delta + \mu)$$
$$-(\delta + \mu)R^* + (\delta + \mu)\frac{(R^*)^2}{R}.$$

We can now write $\frac{dL}{dt} = \phi_1 - \phi_2$, where

$$\phi_1 = \Pi + \alpha V + \delta R + \frac{(S^*)^2}{S}(\eta + \frac{\beta I}{N} + \mu) + \eta S + \frac{(1-p)\beta I(V^*)^2}{NV} + \frac{(\alpha+\mu)(V^*)^2}{V}$$
$$+\frac{\beta S(I^*)^2}{NI} + \frac{(1-p)\beta V(i^*)^2}{NI} + (\omega + \mu + \xi)\frac{(I^*)^2}{I} + \omega I + (\gamma + \mu)\frac{(T^*)^2}{T} + (\delta + \mu)\frac{(R^*)^2}{R}.$$

$$\phi_2 = \frac{(S-S^*)^2}{S}(\eta + \frac{\beta I}{N} + \mu) + \frac{S^*}{S}(\Pi + \alpha V + \delta R) + (\eta + \frac{\beta I}{N} + \mu)S^* + \frac{(V-V^*)^2}{V}(\frac{(1-p)\beta I}{N}$$
$$+(\alpha + \mu)) + \eta S\frac{V^*}{V} + (\frac{(1-p)\beta IV^*}{NV}) + (\alpha + \mu)V^* + \frac{(I-I^*)^2}{I}(-(1-p)\frac{\beta V}{N} + \frac{\beta SI^*}{N} + \frac{(1-p)\beta VI^*}{N}$$
$$+(\omega + \mu + \xi) - \frac{\beta S}{N}) + \frac{\beta SI^*}{N} + \frac{(1-p)\beta VI^*}{N} + (\omega + \mu + \xi)I^* + \frac{(T-T^*)^2}{T}(\gamma + \mu) + \omega I\frac{T^*}{T}$$
$$+(\gamma + \mu)T^* + \frac{(R-R^*)^2}{R}(\delta + \mu) + \frac{R^*}{R}((\delta + \mu)R^*.$$

Since all the parameters used in model (2.1) are non-negative
$\frac{dL}{dt} \leq 0$ for $\phi_1 \leq \phi_2$, and $\frac{dL}{dt} = 0$ if and only if $\phi_1 = \phi_2$ which implies that $\frac{dL}{dt} = 0$ if and only if $S = S^*$, $V = V^*$, $I = I^*$, $T = T^*$, $R = R^*$.

According to Lasalle's invariance principle, the Cholera Equilibrium Point is globally asymptotically stable. This means that the CEP is a stable state that the system will converge to, regardless of the initial conditions. Furthermore, the implication of Theorem 6 is that Cholera will become entrenched and established within the society. In other words, Cholera will become a persistent and endemic disease that will institute itself and continue to spread and affect the population. □

3.11. Bifurcation Analysis

Bifurcation occurs in a dynamical system when gradual changes in the system's parameter values lead to abrupt qualitative or topological shifts in its behavior. In epidemiology, bifurcations are classified into two main types: local and global [25]. For the governing system (2.1), we will designate the effective cholera transmission rate, β, as the bifurcation parameter. Consequently, model (2.1) can be expressed in vector form by renaming the variables as follows:
$S = y_1$, $V = y_2$, $I = y_3$, $T = y_4$, $R = y_5$. That is,

$$\frac{dY}{dt} = G(Y), \tag{3.17}$$

where,

$$Y = (y_1, y_2, y_3, y_4, y_5)^T, G(Y) = (g_1, g_2, g_3, g_4, g_5).$$

Then, model (2.1) becomes

$$\begin{cases} \frac{dy_1}{dt} = (1 - \alpha)\Pi - (\lambda + \mu)y_1 + p\eta y_2 + \delta y_5 = g_1, \\ \frac{dy_2}{dt} = \alpha\Pi - (\eta + \mu)y_2 = g_2, \\ \frac{dy_3}{dt} = \lambda y_1 + (1 - p)\eta y_2 - (\omega + \mu + \xi)y_3 = g_3, \\ \frac{dy_4}{dt} = \omega y_3 - (\gamma + \mu + \xi)y_4 = g_4, \\ \frac{dy_5}{dt} = \gamma y_4 - (\delta + \mu)y_5 = g_5. \end{cases} \tag{3.18}$$

Here, from preceding system of nonlinear equation, choosing β as a bifurcation parameter and setting $R_{eff} = 1$, we have

$$\beta^* = \beta = \omega + \mu + \xi + \frac{\alpha\mu(\omega + \mu + \xi)}{\eta + \mu + \alpha(\eta p - \eta - \mu)}. \tag{3.19}$$

So that the disease-free equilibrium, E_0, is locally stable when $\beta < \beta^*$ and is unstable when $\beta > \beta^*$. The linearized matrix of the system around the disease-free equilibrium E_0 and evaluated at β^* is given by

$$J(E_0, \beta^*) = \begin{bmatrix} -\mu & p\eta & \omega + \mu + \xi & 0 & \delta \\ 0 & -(\eta + \mu) & 0 & 0 & 0 \\ 0 & (1 - p)\eta & 0 & 0 & 0 \\ 0 & 0 & \omega & -(\gamma + \mu + \xi) & 0 \\ 0 & 0 & 0 & \gamma & -(\delta + \mu) \end{bmatrix}$$

The eigenvalues of matrix $J(E_0, \beta^*)$ are $\lambda_1 = -\mu, \lambda_2 = -(\eta+\mu), \lambda_3 = 0, \lambda_4 = -(\gamma+\mu+\xi), \lambda_5 = -(\delta+\mu)$, have negative eigenvalues and one simple zero eigenvalue at $R_0 = 1$ at (E_0, β^*). It follows that $J(E_0, \beta^*)$ have a simple zero eigenvalue and the rest of eigenvalues have negative real parts, which indicates E_0 is a nonhyperbolic equilibrium when $\beta = \beta^*$.

Moreover, let $u = (u_1, u_2, u_3, u_4, u_5)^T$ be the right eigenvector, associated with simple zero eigenvalue and can be obtained by solving equation $J(E_0, \beta^*)u = 0$. Thus, we have

$$J(E_0, \beta^*)u = \begin{bmatrix} -\mu & p\eta & \omega+\mu+\xi & 0 & \delta \\ 0 & -(\eta+\mu) & 0 & 0 & 0 \\ 0 & (1-p)\eta & 0 & 0 & 0 \\ 0 & 0 & \omega & -(\gamma+\mu+\xi) & 0 \\ 0 & 0 & 0 & \gamma & -(\delta+\mu) \end{bmatrix} \begin{bmatrix} u_1 \\ u_2 \\ u_3 \\ u_4 \\ u_5 \end{bmatrix} = \begin{bmatrix} 0 \\ 0 \\ 0 \\ 0 \\ 0 \end{bmatrix}$$

Simplification and rearrangement yields

$$\begin{cases} u_1 = (\frac{(\omega+\mu+\xi)(\gamma+\mu+\xi)}{\mu\omega} + \frac{\delta\gamma}{\delta+\mu})u_4, u_2 = 0, u_3 = \frac{(\gamma+\mu+\xi)u_4}{\omega}, \\ u_4 = \frac{(\delta+\mu)u_5}{\gamma}, u_5 = \frac{\gamma u_4}{\delta+\mu}. \end{cases} \tag{3.20}$$

Also, let $w = (w_1, w_2, w_3, w_4, w_5)$ be the left eigenvector corresponding to simple zero eigenvalue, obtained by setting and solving $w^T J(E_0, \beta^*) = 0$, we have,

$$wJ(E_0, \beta^*) = \begin{bmatrix} w_1 \\ w_2 \\ w_3 \\ w_4 \\ w_5 \end{bmatrix} \begin{bmatrix} -\mu & p\eta & \omega+\mu+\xi & 0 & \delta \\ 0 & -(\eta+\mu) & 0 & 0 & 0 \\ 0 & (1-p)\eta & 0 & 0 & 0 \\ 0 & 0 & \omega & -(\gamma+\mu+\xi) & 0 \\ 0 & 0 & 0 & \gamma & -(\delta+\mu) \end{bmatrix} = \begin{bmatrix} 0 \\ 0 \\ 0 \\ 0 \\ 0 \end{bmatrix}.$$

This gives

$$w_1 = 0, w_2 = \frac{(1-p)\eta w_3}{\eta+\mu}, w_3 = \frac{(\eta+\mu)w_2}{1-p}\eta, w_4 = 0, w_5 = 0. \tag{3.21}$$

In order that the required conditions $u.w = 1$, the product give,

$$u_1 w_1 + u_2 w_2 + u_3 w_3 + u_4 w_{14} + u_5 w_5 = 1. \tag{3.22}$$

Again substituting the corresponding components in the preceding equation, we have

$$\frac{u_4 w_2(\gamma+\mu+\xi)}{(1-p)\eta} = 1. \tag{3.23}$$

Thus, the preceding equality is satisfied if we choose

$$u_4 = \frac{1}{(\gamma+\mu+\xi)(\eta+p)}, w_2 = (1-p)\eta. \tag{3.24}$$

Utilizing the center manifold theorem in bifurcation theory, as outlined by Castillo-Chavez and Song in Carr [26], we determine the parameters A_1 and A_2 as follows:
we compute the parameters A_1 and A_2 as

$$
\begin{cases}
A_1 = \sum_{k,i,j=1}^{4} w_k u_i u_j \frac{\partial^2 f_k}{\partial x_i \partial x_j}(E_0, \beta^*) = \sum_{i,j=1}^{4} w_3 u_i u_j \frac{\partial^2 f_3}{\partial x_i \partial x_j}(E_0, \beta^*), \\
\quad = w_3 u_1^2 \frac{\partial^2 g_3}{\partial y_1^2}(E_0, \beta^*) + w_3 u_2^2 \frac{\partial^2 g_3}{\partial y_2^2}(E_0, \beta^*) \\
\quad + w_3 u_3^2 \frac{\partial^2 g_3}{\partial y_3^2}(E_0, \beta^*) + w_3 u_4^2 \frac{\partial^2 g_3}{\partial y_4^2}(E_0, \beta^*) + w_3 u_5^2 \frac{\partial^2 g_3}{\partial y_5^2}(E_0, \beta^*), \\
\quad = -\frac{2\beta y_1}{(y_1+y_2)^2} = \frac{-2\beta b \mu(\eta+\mu)}{(b+\mu\alpha\Pi)^2} < 0, \\
A_2 = \sum_{k,i=1}^{4} w_k u_i \frac{\partial^2 f_k}{\partial x_i \partial \beta^*}(E_0, \beta^*), \\
\quad = w_1 u_1 \frac{\partial^2 g_1}{\partial Y_1 \partial \beta^*}(E_0, \beta^*) + w_2 u_2 \frac{\partial^2 g_2}{\partial Y_2 \partial \beta^*}(E_0, \beta^*) + w_3 u_3 \frac{\partial^2 g_3}{\partial Y_3 \partial \beta^*}(E_0, \beta^*) + w_4 u_4 \frac{\partial^2 g_4}{\partial Y_4 \partial \beta^*}(E_0, \beta^*) \\
\quad + w_5 u_5 \frac{\partial^2 g_5}{\partial Y_5 \partial \beta^*}(E_0, \beta^*), \\
\quad = w_3 u_3 \frac{\partial^2 g_3}{\partial Y_3 \partial \beta^*}(E_0, \beta^*) = w_3 u_3 \frac{y_1}{(y_1+y_2)^2} = w_3 u_3 \frac{\Pi b \mu(\eta+\mu)}{(b+\mu\alpha\Pi)^2} = \frac{\eta^2(\eta+\mu)}{\omega(\eta+p)} > 0,
\end{cases}
\tag{3.25}
$$

$$
\text{where },\ b = \eta + \mu + \alpha(\eta p - \eta - \mu).
$$

We employ the center manifold theory as in [18] to compute the coefficients $A_i (i = 1, 2)$ in equation (3.26), thereby finalizing the bifurcation analysis. This involves determining the nonzero second-order partial derivatives of $f_k (k = 1, ..., 5)$ with respect to $y_i (i = 1, ..., 5)$ around the disease-free equilibrium.

The center manifold theory allows us to simplify the analysis of the dynamical system by reducing the dimension of the system around the bifurcation point. By computing the coefficients A_i, we can classify the type of bifurcation and predict the qualitative changes in the system's behavior as the bifurcation parameter, in this case the effective cholera transmission rate β varies.

$$
\begin{cases}
\frac{\partial^2 g_1}{\partial y_1^2} =, \frac{\partial^2 g_1}{\partial y_1 \partial y_2} = \frac{\partial^2 g_1}{\partial y_2 \partial y_1} =, \frac{\partial^2 g_1}{\partial y_2^2} = \frac{\partial^2 g_1}{\partial y_4 \partial y_2} = \frac{\partial^2 g_1}{\partial y_2 \partial y_4} = 0, \frac{\partial^2 g_1}{\partial y_3 \partial y_2} = \frac{\partial^2 g_1}{\partial y_2 \partial y_3} = \frac{\beta y_1}{(y_1+y_2)^2}, \\
\frac{\partial^2 g_1}{\partial y_3^2} = \frac{2\beta y_1}{(y_1+y_2)^2}, \frac{\partial^2 g_1}{\partial y_1 \partial y_3} = \frac{\partial^2 g_1}{\partial y_3 \partial y_1} = \frac{-\beta}{y_1+y_2} + \frac{\beta y_1}{(y_1+y_2)^2}, \frac{\partial^2 g_1}{\partial y_4 \partial y_3} = \frac{\partial^2 g_1}{\partial y_3 \partial y_4} = \frac{\beta y_1}{(y_1+y_2)^2}, \\
\frac{\partial^2 g_1}{\partial y_4^2} = \frac{\partial^2 g_1}{\partial y_1 \partial y_4} = \frac{\partial^2 g_1}{\partial y_4 \partial y_1} = \frac{\partial^2 g_2}{\partial y_2^2} = \frac{\partial^2 g_2}{\partial y_1 \partial y_2} = \frac{\partial^2 g_2}{\partial y_2 \partial y_1} = \frac{\partial^2 g_2}{\partial y_3^2} = \frac{\partial^2 g_2}{\partial y_3 \partial y_2} = \frac{\partial^2 g_2}{\partial y_2 \partial y_3} = \frac{\partial^2 g_2}{\partial y_4 \partial y_2} = 0, \\
\frac{\partial^2 g_2}{\partial y_2 \partial y_4} = \frac{\partial^2 g_2}{\partial y_3^2} = \frac{\partial^2 g_2}{\partial y_1 \partial y_3} = \frac{\partial^2 g_2}{\partial y_3 \partial y_1} = \frac{\partial^2 g_2}{\partial y_4 \partial y_3} = \frac{\partial^2 g_2}{\partial y_3 \partial y_4} = \frac{\partial^2 g_2}{\partial y_4^2} = 0, \\
\frac{\partial^2 g_3}{\partial y_3 \partial y_2} = \frac{-\beta y_1}{(y_1+y_2)^2}, \frac{\partial^2 g_3}{\partial y_4 \partial y_2} = \frac{\partial^2 g_3}{\partial y_3^2} = \frac{-\beta y_1}{(y_1+y_2)^2}, \frac{\partial^2 g_3}{\partial y_4 \partial y_3} = -\frac{\beta y_1}{(y_1+y_2)^2}, \frac{\partial^2 g_3}{\partial y_1 \partial y_3} = \frac{\beta}{y_1+y_2} - \frac{\beta y_1}{(y_1+y_2)^2}, \\
\frac{\partial^2 g_2}{\partial y_1 \partial y_4} = \frac{\partial^2 g_2}{\partial y_4 \partial y_1} = \frac{\partial^2 g_3}{\partial y_1^2} = \frac{\partial^2 g_3}{\partial y_1 \partial y_2} = \frac{\partial^2 g_3}{\partial y_2^2} = \frac{\partial^2 g_3}{\partial y_4^2} = \frac{\partial^2 g_4}{\partial y_1 \partial y_4} = 0, \\
\frac{\partial^2 g_5}{\partial y_1^2} = \frac{\partial^2 g_5}{\partial y_1 \partial y_2} = \frac{\partial^2 g_5}{\partial y_2^2} = \frac{\partial^2 g_5}{\partial y_3 \partial y_2} = \frac{\partial^2 g_5}{\partial y_4 \partial y_2} = \frac{\partial^2 g_5}{\partial y_3^2} = \frac{\partial^2 g_5}{\partial y_1 \partial y_3} = \frac{\partial^2 g_5}{\partial y_4 \partial y_3} = \frac{\partial^2 g_5}{\partial y_4^2} = \frac{\partial^2 g_5}{\partial y_1 \partial y_4} = 0.
\end{cases}
$$

Also,

$$
\begin{cases}
\frac{\partial^2 g_2}{\partial y_2 \partial \beta^*}(E_0, \beta^*) = 0, \\
\frac{\partial^2 g_3}{\partial y_3 \partial \beta^*}(E_0, \beta^*) = \frac{y_1}{(y_1+y_2)^2}, \\
\frac{\partial^2 g_k}{\partial y_i \partial \beta^*}(E_0, \beta^*) = 0, i \neq 0.
\end{cases}
$$

Since $A_1 < 0$ and $A_2 > 0$, the model exhibits forward bifurcation at $R_{eff} = 1$.

Next, following procedures given in [15], we compute the bifurcation coefficients A_1 and A_2, to identify the direction of bifurcation at $R_{eff} = 1$. Thus, we have

$$
\begin{cases}
A_1 = \sum_{k,i,j=1}^{4} w_k u_i u_j \frac{\partial^2 f_k}{\partial x_i \partial x_j}(E_0, \beta^*) = \sum_{i,j=1}^{4} w_3 u_i u_j \frac{\partial^2 f_3}{\partial x_i \partial x_j}(E_0, \beta^*) = \frac{-2\beta b \mu(\eta+\mu)}{(b+\mu\alpha\Pi)^2} < 0, \\
A_2 = \sum_{k,i=1}^{4} w_k u_i \frac{\partial^2 f_k}{\partial x_i \partial \beta^*}(E_0, \beta^*) = w_3 u_3 \frac{\partial^2 g_3}{\partial Y_3 \partial \beta^*}(E_0, \beta^*) = w_3 u_3 \frac{\partial^2 g_3}{\partial Y_3 \partial \beta^*}(E_0, \beta^*) = w_3 u_3 \frac{y_1}{(y_1+y_2)^2} \\
\quad = w_3 u_3 \frac{\Pi b \mu(\eta+\mu)}{(b+\mu\alpha\Pi)^2} = \frac{\eta^2(\eta+\mu)}{\omega(\eta+p)} > 0.
\end{cases}
\tag{3.26}
$$

Given that all parameters in model (2.1) are non-negative, and additionally w_3 and u_3 are positive, we can deduce that $A_1 < 0$ and $A_2 > 0$. Consequently, following the findings of [11], model (2.1) demonstrates

a supercritical bifurcation as R_{eff} crosses the threshold $R_{eff} = 1$. This implies the existence of a locally asymptotically stable endemic equilibrium point $E_1^* = (S^*, V^*, I^*, T^*, R^*)$ for $R_{eff} > 1$. Drawing on the outcomes of the aforementioned discussion as Fig. 2 and referencing [12], the following theorem is formulated.
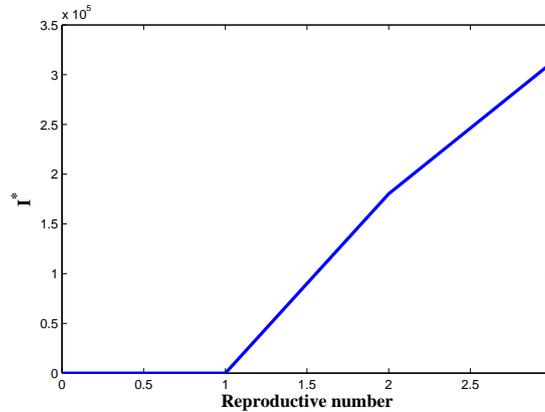

Figure 2: Forward bifurcation of Cholera model

Theorem 3.7. *The trans-critical bifurcation of model (2.1) at $R_0 = 1$ is characterized as a supercritical bifurcation. This implies the presence of a locally asymptotically stable endemic equilibrium point $E_1 = (S^*, V^*, I^*, T^*, R^*)$ for $R_0 > 1$.*

Remark 3.8. Theorem 3.7 indicates that when $R_0 > 1$, even a minor influx of infectious individuals into a fully susceptible population can lead to the sustained presence of cholera within the population.

3.12. Sensitivity Analysis

In this section, we perform the sensitivity analysis of the basic reproductive number. Sensitivity evaluation tells us how crucial every parameter is to disease transmission. Such facts is essential now no longer simplest for experimental design, however additionally to information assimilation and discount of complex nonlinear models. Sensitivity evaluation is typically used to decide the robustness of model predictions to parameter values, when you consider that there are normally mistakes in facts series and presumed parameter values. It is used to find out parameters that have a high impact on basic reproduction quantity and need to be centered through intervention strategies. The normalized forward sensitivity index of a particular variable, R_0, with respect to a parameter, H, is defined as

$$X_H^{R_0} = \frac{\partial R_0}{\partial H} \times \frac{H}{R_0}. \tag{3.27}$$

It is already shown that the explicit expression of R_0 is given by

$$R_0 = \frac{\beta[\eta + \mu + \alpha(\eta p - \eta - \mu)]}{([\eta + \mu + \alpha(\eta p - \eta - \mu)] + \alpha\mu)(\omega + \mu + \xi)}. \tag{3.28}$$

The normalized forward sensitivity indices of R_0 with respect to parameters in it are given by

$$\begin{cases} X_\beta^{R_0} = \frac{\partial R_0}{\partial \beta} \times \frac{\beta}{R_0} = 1, \\ X_\alpha^{R_0} = \frac{\partial R_0}{\partial \alpha} \times \frac{\alpha}{R_0} = \frac{[(\eta p - \eta - \mu)(\eta + \mu + \eta \alpha p - \eta \alpha) - (\eta + \mu + \alpha \eta p - \eta \alpha - \mu \alpha)(\eta p - \eta)]\alpha}{(\eta + \mu + \eta \alpha p - \eta \alpha - \mu \alpha)(\eta + \mu + \eta \alpha p - \alpha \eta)}, \\ X_\eta^{R_0} = \frac{\partial R_0}{\partial \eta} \times \frac{\eta}{R_0} = \frac{(1 + \alpha p - \alpha)\alpha \mu \eta}{(\eta + \mu + \eta \alpha p - \alpha \eta)(\eta + \mu + \alpha \eta p - \eta \alpha - \mu \alpha)}, \\ X_\xi^{R_0} = \frac{\partial R_0}{\partial \xi} \times \frac{\xi}{R_0} = \frac{-\xi}{(\omega + \mu + \xi)}, \\ X_p^{R_0} = \frac{\partial R_0}{\partial p} \times \frac{p}{R_0} = \frac{(\alpha \eta p)[(\eta + \mu + \alpha \eta p - \alpha \eta) - (\eta + \mu + \alpha \eta p - \alpha \eta - \alpha \mu)]}{(\eta + \mu + \eta \alpha p - \alpha \eta)(\eta + \mu + \alpha \eta p - \eta \alpha - \mu \alpha)}, \\ X_\omega^{R_0} = \frac{\partial R_0}{\partial \omega} \times \frac{\omega}{R_0} = \frac{-\omega}{(\omega + \mu + \xi)}. \end{cases} \tag{3.29}$$

Table 1: Sensitivity indices table

parameters Symbol	Description	Sensitivity indices
β	Rate of infection transmission	1
p	The efficacy of the vaccine available	0.0054
η	The percapita rate of becoming infectious	0.0002
ξ	Cholera -induced death rate	-0.768
ω	Rate of infected individuals join treatment class	-0.231
α	Fraction of recruits who are high risk	-0.00085

The interpretation of the sensitivity indices given in Table 1 is as follows. Those parameters that have positive sensitivity indices (β, p, η) have a big contribution to the expansion of cholera disorder with inside the human populace if their values are expanded via way of means of preserving the relaxation of parameters constant. And those parameters that have negative sensitivity indices (α, ω, ξ) show a great effect in bringing down the ailment from the populace if their values are reduced via way of means of preserving the relaxation of parameters constant. Due to the reason that R_0 (basic reproductive number) increases as its parameter cost will increase, the common wide variety of secondary contamination will increase withinside the population; and R_0 decreases as its parameter value decreases, which means that the average number of secondary contamination decreases with inside the human population and illustrated as Fig. 3.
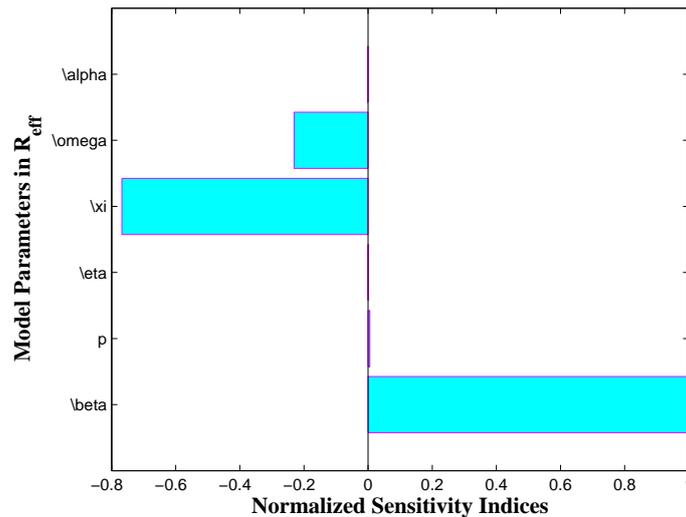

Figure 3: Sensitivity indices of basic reproduction number R_0

4. Optimal Control Model

The aim of this section is to extend model equation (2.1) into an optimal control problem. The controls are defined as follows;

1. u_1 represents a prevention effort that protects susceptible individuals from contracting the disease. This could involve measures such as improving water and sanitation infrastructure, promoting hygiene practices, or implementing vaccination programs to reduce the likelihood of susceptible individuals becoming infected.

2. u_2 represents a treatment effort that aims to minimize the impact of infections by treating infectious individuals. This could involve improving access to medical care, providing timely diagnosis and treatment of cholera cases, or implementing interventions that reduce the duration or severity of the infectious period.

After incorporating, u_1 and u_2 in cholera model (2.1), we obtain the following optimal control model:

$$
\begin{cases}
\frac{dS}{dt} = (1-\alpha)\Pi - (1-u_1)\frac{\beta I}{N}S - \mu S + p\eta V + \delta R, \\
\frac{dV}{dt} = \alpha\Pi - (\eta + \mu)V, \\
\frac{dI}{dt} = (1-u_1)\frac{\beta I}{N}S + (1-p)\eta V - (\omega + \mu + \xi)I, \\
\frac{dT}{dt} = \omega I - (\gamma + u_2)T - (\mu + \xi)T, \\
\frac{dR}{dt} = (\gamma + u_2)T - (\delta + \mu)R,
\end{cases}
\tag{4.1}
$$

with $\lambda = \frac{\beta I}{N}$ and initial condition $S(0) > 0, V(0) \geq 0, I(0) \geq 0, T(0) \geq 0, R(0) \geq 0$. A bounded Lebesgue measurable control set is represented as:

$$
\Omega = \{(u_1, u_2), 0 \leq u_i \leq u_{imax}, i = 1, 2\} \text{ and } t \in [0, T].
$$

The main objective is to minimize the number of infected and treatment population while minimizing the rate of interventions u_1 and u_2 on a fixed time period T.

Therefore, the optimal control problem for the model equation (4.1) is to minimize the objective function;

$$
J(u) = min \int_0^T [M_1 I + M_2 T + \frac{1}{2}\sum_{i=1}^2 w_i u_i^2(t)]dt,
\tag{4.2}
$$

where $i = 1, 2$ and $M_1, M_2, \frac{w_1}{2}$ and $\frac{w_2}{2}$ are positive weights that balance the size of the integrand terms to reduce the dominance of any of the term in the integral. The constants w_1 and w_2 measures the cost or effort required for the implementation of each of the two control measures adopted while M_1 and M_2 measures the relative importance of reducing the associated classes on the spread of the disease. The parameter T is the duration of time in years of prevention and treatment progress. Thus, we need to find the optimal controls $u^* = (u_1^*, u_2^*)$ such that;

$$
J(u^*) = min_u J(u_1, u_2).
$$

Hence, the basic setup of the optimal control problem is to check the existence and uniqueness of the optimal controls and to characterize them.

4.1. Existence of an Optimal Control

Theorem 4.1. *Consider the objective function $J(u)$ as in (4.2) with the set of admissible control Ω subject to the system ,then there exist an optimal control $(u_1^*, u_2^*) \in \Omega$ such that*

$$
J(u_1^*, u_2^*) = min(u_1, u_2 \in \Omega)J(u_1, u_2)
$$

the subsequent situations are satisfied.

Let the control set

$$
\Omega = [0, 1]^2, v = (u_1, u_2) \in \Omega, \chi = (S^*, V^*, I^*, T^*, R^*)
$$

and $g(t, \chi, v)$ the right hand side of state system (4.1), is given by

$$
g(t, \chi, v) =
\begin{cases}
\frac{dS}{dt} = (1-\alpha)\Pi - (1-u_1)\frac{\beta I}{N}S - \mu S + p\eta V + \delta R, \\
\frac{dV}{dt} = \alpha\Pi - (\eta + \mu)V, \\
\frac{dI}{dt} = (1-u_1)\frac{\beta I}{N}S + (1-p)\eta V - (\omega + \mu + \xi)I, \\
\frac{dT}{dt} = \omega I - (\gamma + u_2)T - (\mu + \xi)T, \\
\frac{dR}{dt} = (\gamma + u_2)T - (\delta + \mu)R.
\end{cases}
\tag{4.3}
$$

The proof is based on the following assumption and by Fleming and Rishel's theorem [23].

1. The set of controls and corresponding state variables is nonempty.
2. The admissible control set Ω is convex and closed.
3. All the right hand sides of equations of system (2.1) are continuous, bounded above by a sum of bounded control and state, and can be written as a linear function of u, v, and w with coefficients depending on time and state.
4. The integrand of the objective functional $M_1 I + M_2 T + \frac{1}{2} W_1 u_1^2 + \frac{1}{2} W_2 u_2^2$ is convex.
5. The integrand of the objective functional is bounded below by

$$M_1 I + M_2 T + \tfrac{1}{2} W_1 u_1^2 + \tfrac{1}{2} W_2 u_2^2 \geq c_1 + c_2 |u_1|^\tau + c_3 |u_2|^\tau.$$

where $c_1, c_2, c_3 > 0$ and $\tau > 1$.

Proof. The non trivial requirement on the set of admissible controls and the set of end conditions are followed by [3] theorem.

Condition 1: Using theorem of Picard-Lindelof [36], if $g(t, \chi, \upsilon)$ is bounded, continuous and Lipschitz in the state variables, then there exists a unique solution corresponding to every admissible control Ω. Hence, for every $u_i \in \Omega$ and the state variables, we have

$$0 \leq N(t) \leq \frac{\Pi}{\mu}, \tag{4.4}$$

and non empty by model assumption. Furthermore, with the bounded done in (3.4) it implies that the state variable is continuous and bounded. Additionally, the partial derivative $\frac{\partial g}{\partial x}$ exist and finite (i.e. are all continuous). Therefore, there exists a unique solution (S, V, I, T, R) that satisfies the initial conditions. Hence, the set of controls and the corresponding state variables is nonempty and condition 1 is satisfied.

Condition 2: Assume that $u_1, u_2 \in \Omega$ such that $||u_1|| \leq 1, ||u_2|| \leq 1$. Now, let us take any controls $u_1, u_2 \in \Omega$ and $\lambda \in [0, 1]$, then $0 \leq \lambda u_1 + (1 - \lambda) u_2$. Additionally, we observe that

$$||\lambda u_1|| = \lambda ||u_1|| \leq \lambda \text{ and}$$
$$||(1 - \lambda) u_2|| = (1 - \lambda) ||u_2|| \leq (1 - \lambda) \text{ since}, ||u_i|| \leq 1. \text{ Then for any } \lambda \in [0, 1],$$
$$||\lambda u_1 + (1 - \lambda) u_2||$$
$$\leq ||\lambda u_1|| + ||(1 - \lambda) u_2||$$
$$= \lambda ||u_1|| + (1 - \lambda) ||u_2||$$
$$< \lambda + (1 - \lambda) = 1$$

Hence, $0 \leq \lambda u_1 + (1 - \lambda) u_2 \leq 1$, for all $u_1, u_2 \in \Omega$ and $\lambda \in [0, 1]$.

Therefore, the control space $u = \{u = (u_1, u_2), 0 \leq u_i \leq u_i max, i = 1, 2\}$ and $t \in [0, T]$ is convex and closed by definition.

The existence of the result in (3.4) for the equation of system (2.1) with bounded coefficients is used to hold the condition under (3.2). The control set u is convex and is closed by definition. The RHS of the state variables in (2.1) holds. Condition (3.4) as the state solutions is a priori bounded. The integrand of the objective functional $M_1 I + M_2 T + \frac{1}{2} \sum_{i=1}^{2} w_i u_i^2(t)$ is clearly concave on u. Finally, $n_1 > 0, n_2 > 0$, and $\beta > 0$.

$$M_1 I + M_2 T + \frac{1}{2} \sum_{i=1}^{2} w_i u_i^2(t) \leq n_1 - n_2 (u_1^2, u_2^2)^{\frac{\alpha}{2}}. \tag{4.5}$$

The state variables are bounded. Hence, there exists an optimal control (u_1, u_2) that minimizes the objective functional $J(u_1, u_2)$. $\qquad\square$

4.2. Hamiltonian and Optimality Condition

The necessary condition for the optimal is obtained using the principle in [29]. Thus, the Hamiltonian (H) is defined by the following equation:

$$Hs(y, u_1(t), u_2(t), \lambda_j, t) = L(I, T, u_1(t), u_2(t)) + \lambda_1 \frac{dS}{dt} + \lambda_2 \frac{dV}{dt} + \lambda_3 \frac{dI}{dt} + \lambda_4 \frac{dT}{dt} + \lambda_5 \frac{dR}{dt}, \qquad (4.6)$$

where,

$$L(I, T, u_1(t), u_2(t)) = M_1 I + M_2 T + \tfrac{1}{2} w_1 u_1^2(t) + \tfrac{1}{2} w_2 u_2^2(t),$$

are the adjoint variable functions to be determined suitably by applying Pontryagin's maximal principle.

Theorem 4.2. *For an optimal control set u_1,u_2 that minimizes J over u, there is an adjoint variables, $\lambda_1, \lambda_2, \lambda_3, \lambda_4, \lambda_5$ such that:*

$$\begin{cases} \frac{d\lambda_1}{dt} = \lambda_1 [\frac{(1-u_1)\beta I}{N} + \mu] - \lambda_3 \frac{(1-u_1)\beta I}{N}, \\ \frac{d\lambda_2}{dt} = -\lambda_1(\eta p) + \lambda_2(\eta + \mu) - \lambda_3(1-p)\eta, \\ \frac{d\lambda_3}{dt} = -M_1 + \lambda_1 \frac{(1-u_1)\beta I}{N} - \lambda_3 \frac{(1-u_1)\beta I}{N} + \lambda_3(\omega + \mu + \xi) - \lambda_4\omega, \\ \frac{d\lambda_4}{dt} = -M_2 + \lambda_4(\gamma + u_2 + \mu + \xi) - \lambda_5(\gamma + u_2), \\ \frac{d\lambda_5}{dt} = -\lambda_1\delta + \lambda_5(\delta + \mu), \end{cases} \qquad (4.7)$$

with transversality conditions, $\lambda_i(t_f) = 0, i = 1, ..., 5$.
Furthermore, we obtain the control set (u_1^*, u_2^*) characterized by

$$u_1(t) = \frac{\beta SI(\lambda_3 - \lambda_1)}{N w_1},$$
$$u_2(t) = \frac{(\lambda_4 - \lambda_5)}{w_2}.$$

Proof. The form of the adjoint equation and transversality conditions are great results from Pontryagin's maximum principle[18]. We differentiate the Hamiltonian (4.6) with respect to states S, V, I, T, and R, respectively, and then the adjoint system can be written as

$$\begin{cases} \frac{d\lambda_1}{dt} = -\frac{\partial H}{\partial S} = \lambda_1 [(1-u_1)\frac{\beta I}{N} + \mu] - \lambda_3(1-u_1)\frac{\beta I}{N}, \\ \frac{d\lambda_2}{dt} = -\frac{\partial H}{\partial V} = -\lambda_1(\eta p) + \lambda_2(\eta + \mu) - \lambda_3(1-p)\eta, \\ \frac{d\lambda_3}{dt} = -\frac{\partial H}{\partial I} = -M_1 + \lambda_1(1-u_1)\frac{\beta S}{N} - \lambda_3(1-u_1)\frac{\beta S}{N} + \lambda_3(\omega + \mu + \xi) - \lambda_4\omega, \\ \frac{d\lambda_4}{dt} = -\frac{\partial H}{\partial T} = -M_2 + \lambda_4(\gamma + u_2 + \mu + \xi) - \lambda_5(\gamma + u_2), \\ \frac{d\lambda_5}{dt} = -\frac{\partial H}{\partial R} = -\lambda_1\delta + \lambda_5(\delta + \mu). \end{cases}$$

Similarly via way of technique of following the approach of [1], to get the controls, we solved the equation, $\frac{\partial H}{\partial u_i} = 0$ at u_i^*, for $i = 1, 2$ and obtained:

$$u_1(t) = \frac{\beta SI(\lambda_3 - \lambda_1)}{N w_1},$$
$$u_2(t) = \frac{(\lambda_4 - \lambda_5)}{w_2}.$$

When we write by using standard control arguments involving the bounds on the controls, we conclude:

$$u_1^* = \begin{cases} \phi_1 & if \, 0 < \phi_1 < 1, \\ 0 & if \, \phi_1 < 0, \\ 1 & if \, \phi_1 \geq 1. \end{cases} \qquad u_2^* = \begin{cases} \phi_2 & if \, 0 < \phi_2 < 1, \\ 0 & if \, \phi_2 < 0, \\ 1 & if \, \phi_2 \geq 1. \end{cases}$$

In compact notation

$$\begin{cases} u_1^*(t) = max\left\{0, min\left\{(1, \frac{\beta SI(\lambda_3-\lambda_1)}{Nw_1})\right\}\right\}, \\ u_2^*(t) = max\left\{0, min\left\{(1, \frac{(\lambda_4-\lambda_5)}{w_2}\right\}\right\}. \end{cases}$$

Then the optimality system is formed from the optimal control system (the state system) and the adjoint variable device thru incorporating the characterized manipulate set and initial and transversal condition.

$$\begin{cases} \frac{dS}{dt} = (1-\alpha)\Pi - (1-u_1^*)\frac{\beta I}{N}S - \mu S + p\eta V + \delta R, \\ \frac{dV}{dt} = \alpha\Pi - (\eta+\mu)V, \\ \frac{dI}{dt} = (1-u_1^*)\frac{\beta I}{N}S + (1-p)\eta V - (\omega+\mu+\xi)I, \\ \frac{dT}{dt} = \omega I - (\gamma+u_2^*)T - (\mu+\xi)T, \\ \frac{dR}{dt} = (\gamma+u_2^*)T - (\delta+\mu)R, \\ \frac{d\lambda_1}{dt} = \lambda_1[(1-u_1^*)\frac{\beta I}{N}+\mu] - \lambda_3(1-u_1^*)\frac{\beta I}{N}, \\ \frac{d\lambda_2}{dt} = -\lambda_1(\eta p) + \lambda_2(\eta+\mu) - \lambda_3(1-p)\eta, \\ \frac{d\lambda_3}{dt} = -M_1 + \lambda_3(\omega+\mu+\xi) - \lambda_4\omega, \\ \frac{d\lambda_4}{dt} = -M_2 + \lambda_4(\gamma+u_2^*+\mu+\xi) - \lambda_5(\gamma+u_2^*), \\ \frac{d\lambda_5}{dt} = -\lambda_1\delta + \lambda_5(\delta+\mu). \end{cases} \quad (4.8)$$

$$\lambda_i(t_f) == 0, i = 1, ..., 5, S_0 = S_0, V_0 = V_0, I_0 = I_0, T_0 = T_0, R_0 = R_0.$$

□

5. Numerical Results and Discussion

In this section, we perform some numerical simulation on the basic model (2.1) and the resulting optimality system consisting of the state equations (4.8) and the adjoint system (4.7). We make use of the parameter values given in Table 2 for the simulation. Since the state system (2.1) has initial conditions and the adjoint systems (4.7) have final conditions, we solve the state system using a forward fourth-order Runge-kutta method and resolve the adjoint system the use of a Backward fourth-order Runge-Kutta method. The solution iterative scheme entails making a guess of the controls and use the guess to solve the state system. The initial guess of the control together with the solution of the state systems is used to solve the adjoint systems. The controls are then updated the usage of a convex combination of the previous controls and the values acquired the usage of the characterizations. The updated controls are then used to duplicate the solution of the state and adjoint systems. This process is repeated until the values in the current iteration are close enough to the previous iteration values [3].

5.1. Numerical Simulation of the Autonomous System

In this section, numerical simulation study of model equations (2.1) is carried out R2015b with ODE45 solver. To conduct using the software MATLAB the study, a set of physically meaningful values are assigned to the model parameters. The values are either taken from assumed or literature on the basis of reality. Using parameter values in Table 2 and the starting conditions $S(0) = 6000, V(0) = 3000, I(0) = 200, T(0) = 80, R(0) = 800$ in the model equations (2.1) and a simulation study is conducted and the results are given in the following Figures. As shown in Fig. 4 as the value of β, ω, η decrease cholera disease goes down by keeping other parameter value constant. Additionally we observe form Fig. 4 as the value of p increase by keeping other parameter constant the infection decrease in the population.
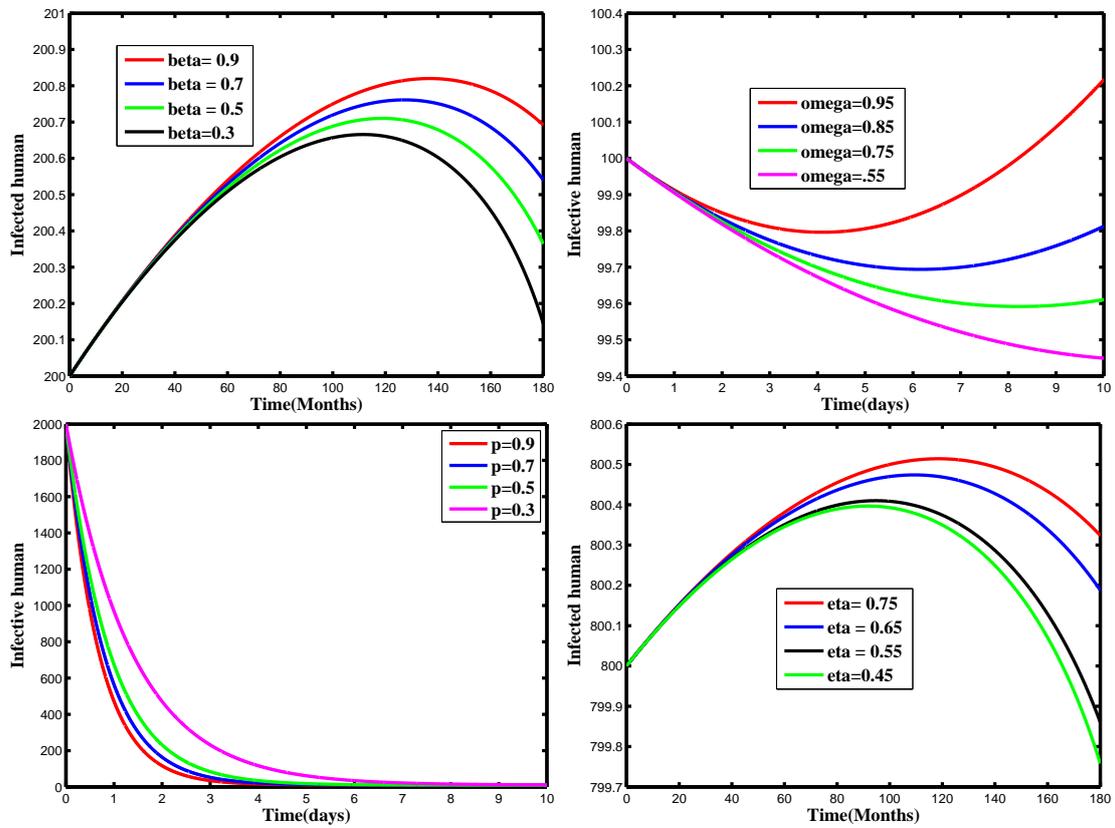
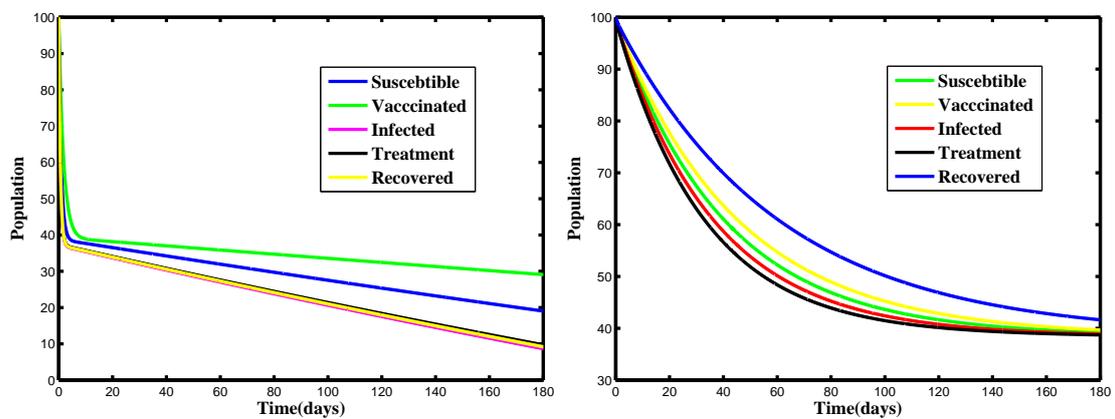Figure 4: Parameters that have a great effect in bringing down the infection

Figure 5: Simulation of local stability and global stability of all equilibrium

Table 2: Parameter values for Cholera disease model

parameters	Description	Value	Source
Π	Recruitment rate	0.0013	[3]
α	Fraction of recruits who are high risk	0.011	Estimated
μ	Natural death rate of human	0.548	[29]
β	Rate of infection transmission	0.0035	Assumed
p	The efficacy of the vaccine available	0.0002	Assumed
η	The percapita rate of becoming infectious	0.005	[29]
ξ	Cholera-induced death rate	0.015	[29]
ω	Rate of infected individuals join treatment class	0.0045	Estimated
γ	Rate of recovery using the available cholera treatment	0.3	Estimated
δ	Rate of recovery after losing their immunity	0.005	Estimated

5.2. Simulation of the Optimal Control Problem

Using different combinations of the controls such as one control only at a time and also all controls at a time, that we analyse and compare numerical results from simulations with the following scenarios.

1. Using prevention effort (u_1) of susceptible without treatment ($u_2 = 0$).
2. Using treatment effort (u_2) without prevention ($u_1 = 0$).
3. Using prevention (u_1) and treatment (u_2).

We used $M_1 = 400, M_2 = 180, w_1 = 4$,and $w_2 = 4$ for simulation of cholera model with optimal control and also for cost-effectiveness analysis. Additionally we used $S(0) = 9400, V(0) = 3200, I(0) = 250, T(0) = 200, R(0) = 200$ as initial values.

Case 1 Control with Prevention Only

In this sub-section the simulation result of the optimality system with preventive intervention only is displayed graphically. In Fig. 5 show it is clearly observed that the decrease of infectious due to implementation of prevention. This can be attribute the fact that prevention minimizes the rate of joining of individuals in to infective as well as treatment compartments. This implies that, optimized prevention reduces the burden of the infection of cholera.
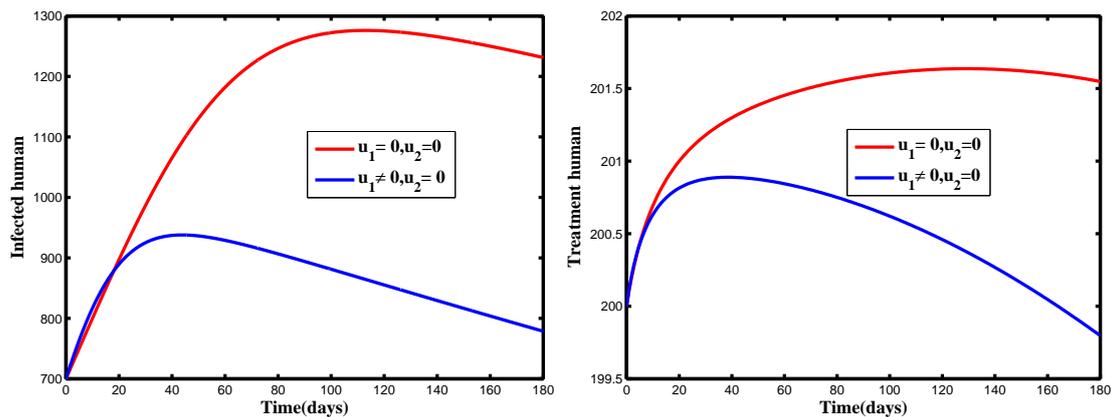

Figure 6: Simulations of optimality system with prevention only

Case 2 Control with Treatment Only

Here, treatment of infectious population is used as the only intervention strategy. Fig. 6 shows that the number of infective together with the treatment humans goes down within the specified time period. Hence, this strategy also works well in eradicating the disease from community.
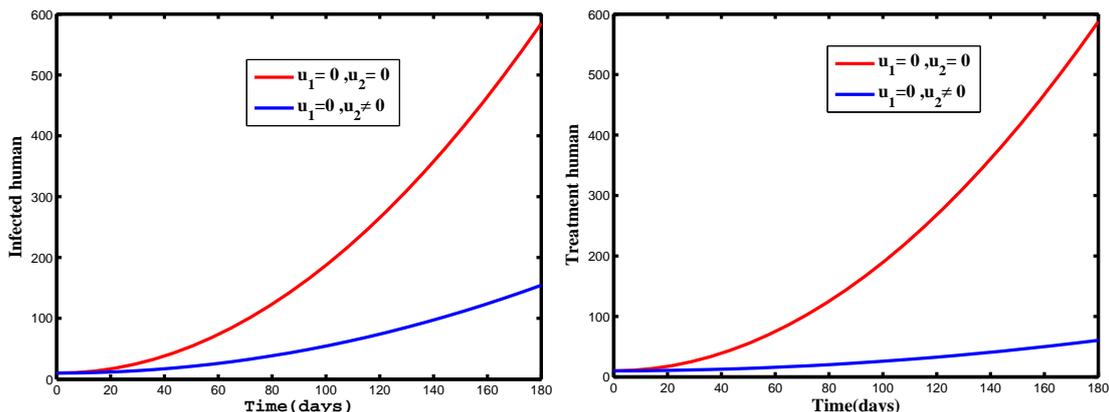
Figure 7: Simulations of optimality system with treatment only

Case 3 Control with Prevention and Treatment

We used prevention and treatment as intervention strategy and in Fig. 7 it is observed that, the number of infective and also treatment goes down in the specified time due the strategy. Therefore, this strategies is effective in eradicating the disease from the community in a specified period of time.
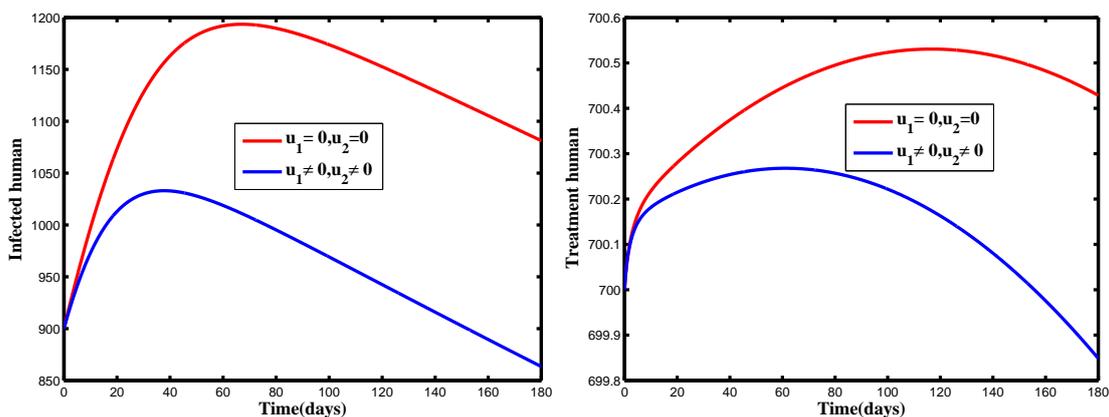

Figure 8: Simulations of optimality system with prevention and treatment interventions
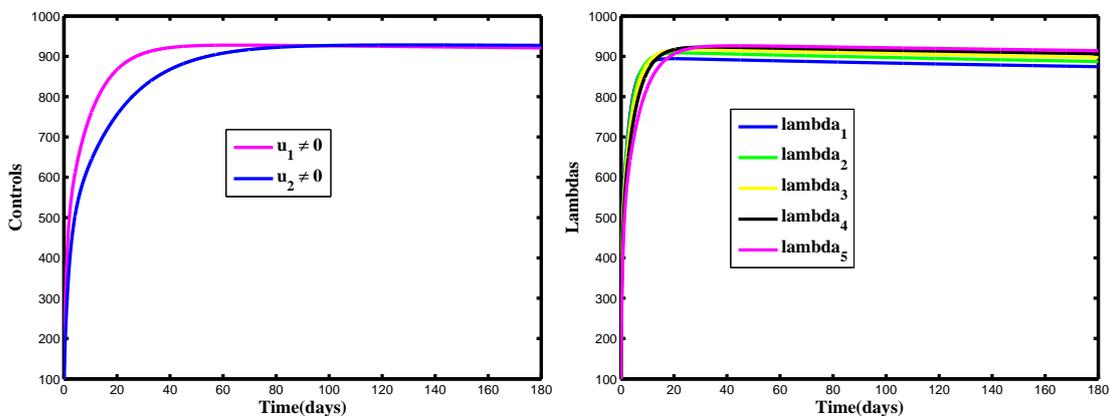

Figure 9: Simulations of controls and adjoint system

5.3. Cost-Effectiveness Analysis

In this section, we have identified a strategy that is profitable compared to other strategies. To obtain this strategy, we used the method of incremental cost-effectiveness ratio (ICER), which is done by dividing the difference of costs between two strategies to the difference of the total value of their infections averted. This approach was defined as follows:

$$ICER(A) = \frac{\text{Cost of strategy A-Cost of Strategy B}}{\text{Total infections saved by Strategy A-Total infections saved by Strategy B}}.$$

Applying one intervention only might to be effective to eradicate the disease from the community. Therefore, we analysed strategies that used more than one intervention method. In Table 3 we obtain the total number of infectious averted and total cost for the implemented strategies. To find the total cost for the implemented strategies we used the cost function given by $\frac{1}{2}M_1u_1^2(t)$, and $\frac{1}{2}M_2u_2^2(t)$ over time. We used the parameter values in Table 2. and to apply $ICER$ technique first we ordered the intervention strategies for pairwise comparison as in Table 3 from A to C with increasing order of effectiveness. First we in comparison

Table 3: Number of infectious averted and total cost of each strategies.

Strategies	Description	Total infectious averted	Total cost ($)	ICER
A	Prevention	112,418	40,798.317	0.363
B	Treatment	118,088	58,869.325	3.187
C	Prevention and Treatment	118565	99,667.642	9.577

the price effectiveness of approach A and B.

$$ICER(A) = \frac{40,798.317}{112,418} = 0.363,$$

$$ICER(B) = \frac{58,869.325 - 40,798.317}{118,088 - 112,418} = 3.187,$$

From ICER (A) and ICER (B) we can see that strategy A saves 0.363 than strategy B. Therefore, we exclude strategy B, because it is a bit expensive and continue to compare strategy A and C.

$$ICER(A) = \frac{40,798.317}{112,418} = 0.363,$$

$$ICER(C) = \frac{99,667.642 - 40,798.317}{118,565 - 112,418} = 9.577.$$

From ICER (A) and ICER (C) we can see that strategy A saves 0.363 than strategy C. Therefore, we exclude strategy C, because it is a bit expensive. Therefore, we conclude that strategy A is the cheapest of all compared strategies, that meant it is the most cost-effective for cholera disease control interventions strategy.

The amount of people averted in strategies A, B and C in an increasing rank is given in Table 3. We can observe that, from the strategies A and B in Fig. 8, the ICER (A) is less than ICER(B). This implies that strategy B is dominated by strategy A. It means that strategy B is more expensive than strategy A. Thus, we have deleted B from the strategies. For further explanation, we plotted a cost function graph, Fig. 9 that shows applying only one intervention costs the least interims of price but we didn't consider this, due to the reason that a single intervention is not effective to eradicate the disease. Additionally, the figure indicates that, applying all the two intervention at once is the high expensive of all the applied intervention strategies. From the strategies A and B with their comparison in Table 3, we can observe that ICER (A) is less than ICER (B). This implies that strategy A is dominated by strategy B. It means that strategy B is more expensive than strategy A. Thus, we have deleted B from the comparison strategies. Then again re-calculate the ICER for the remaining comparison strategies A and C as given in Table 3
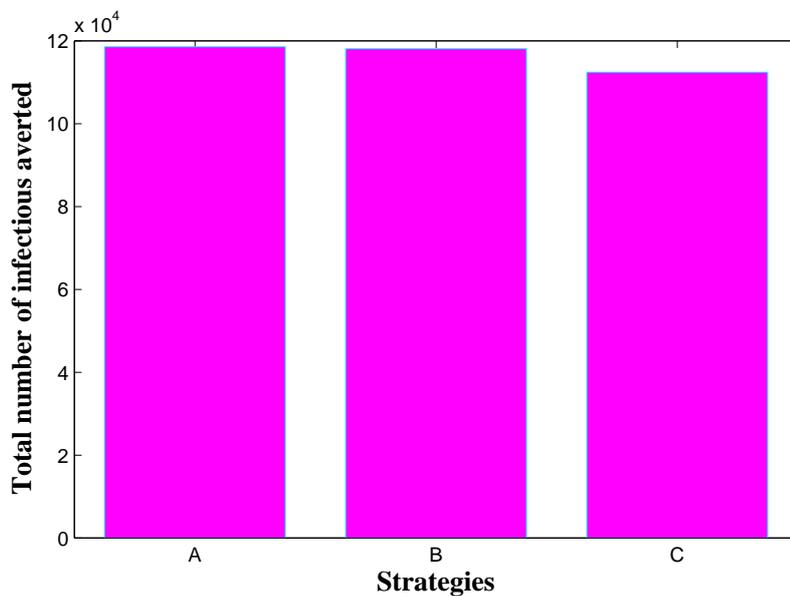
Figure 10: Total infectious averted plots indicating the effect of control strategies A, B, and C
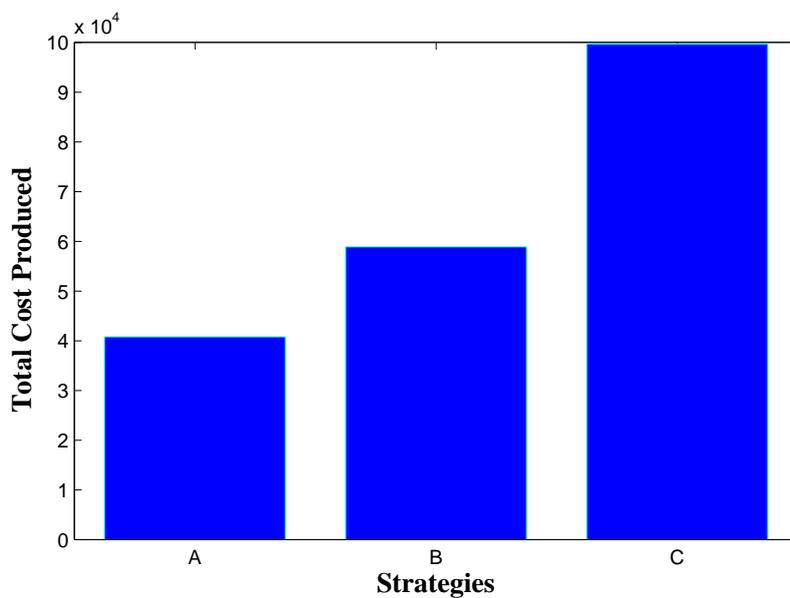

Figure 11: The objective functional plots indicating the effect of control strategies A, B, and C
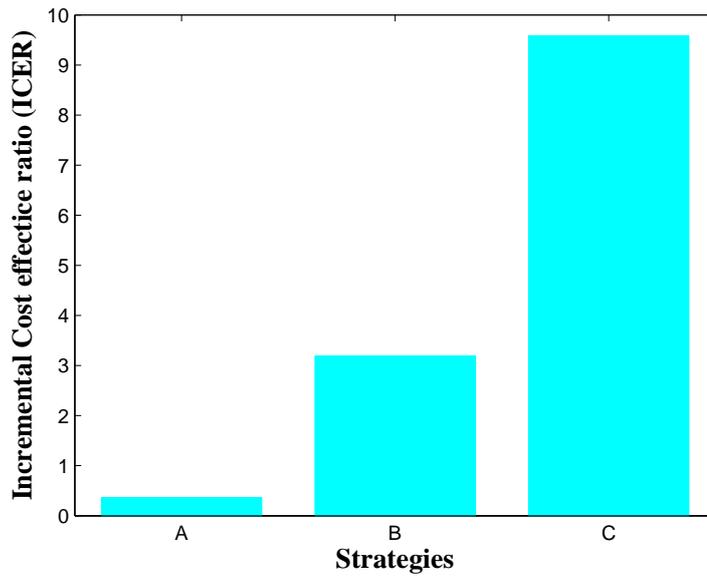
Figure 12: Incremental cost effective ration (ICER) plots indicating the effect of control strategies A, B, and C

6.   Discussions and Conclusions

In this study, we analyzed a deterministic mathematical model of the cholera vaccine epidemic with an optimal control model. We first identified the possible region in which the model is epidemiologically and mathematically well-posed. Then, the basic reproduction number with respect to the disease-free equilibrium is computed using the next-generation matrix method. We then determined both the local and global stability of the disease-free equilibrium point based on the basic reproduction number. By handling the Jacobian matrix, Metzler's matrix, and the Lyapunov method, respectively, we show that the disease-free equilibrium point is both locally and globally stable if the basic reproduction number is below unity. The endemic equilibrium point exists when the basic reproduction number is greater than unity. The analysis of the sensitivity of the model is also described.

The model was extended to the problem of optimal control using two controls, namely personal protection and treatment of infection, for reducing cholera disease. Furthermore, with all controls, the optimal control model satisfies Pontryagin's minimum principle. The result of the numerical simulations shows that every control factor considered in the simulation helped to lower cholera infections.

The authors declare that this manuscript is not yet complete because the model does not fit real cholera data. It is a theoretical discussion with different assumptions on the parameters and initial state variables. Therefore, we recommend that interested researchers apply parameter estimation to the cholera disease model for further novelty.

Data availability

The data we used for this study are from respective published and cited articles.

References

[1] World Health Organization, *Vaccine-preventable diseases surveillance standards*, (2019). 1, 4.2

[2] A. Ouakka, A. Elazzouzi and Z. Hammouch, An SVIQR model with vaccination-age, general nonlinear incidence rate and relapse: Dynamics and simulations, *International Journal of Biomathematics* **18**(2) (2025), 2350092. 1

[3] G. T. Tilahun, W. A. Woldegerima and A. Wondifraw, Stochastic and deterministic mathematical model of cholera disease dynamics with direct transmission, *Advances in Difference Equations* **2020** (2020), 1–23.

[4] Z. T. Shuai, Cholera models with hyperinfectivity and temporary immunity, *Bulletin of Mathematical Biology* **74**(10) (2012), 2423–2445.

[5] X. Cheng, Y. Wang and G. Huang, Edge-based compartmental modeling for the spread of cholera on random networks: A case study in Somalia, *Mathematical Biosciences* **366** (2023), 109092. 1, 2, 4.1, 5, 2

[6] N. Madani and Z. Hammouch, A new approach combining tangent hyperbolic and logistic sigmoid neural networks to model and solve tumor growth dynamics, *Knowledge-Based Systems* (2025), 114679. 1

[7] T. W. Hartley, Public perception and participation in water reuse, *Desalination* **187**(1–3) (2006), 115–126. 1

[8] J. H. Tien and D. J. Earn, Multiple transmission pathways and disease dynamics in a waterborne pathogen model, *Bulletin of Mathematical Biology* **72** (2010), 1506–1533. 1

[9] A. S. Azman, K. E. Rudolph, D. A. Cummings and J. Lessler, The incubation period of cholera: A systematic review, *Journal of Infection* **66**(5) (2013), 432–438.

[10] C.-J. Chang et al., p53 regulates epithelial–mesenchymal transition and stem cell properties through modulating miRNAs, *Nature Cell Biology* **13**(3) (2011), 317–323.

[11] S. Ali, D. Li, C. Congbin and F. Khan, Twenty-first century climatic and hydrological changes over the Upper Indus Basin, *Environmental Research Letters* **10**(1) (2015), 014007.

[12] J. R. Andrews and S. Basu, Transmission dynamics and control of cholera in Haiti: An epidemic model, *The Lancet* **377**(9773) (2011), 1248–1255. 1

[13] D. Bhattacharya and T. I. Khan, The challenges of structural transformation and progress towards the MDGs in LDCs, *Istanbul Programme of Action for the LDCs* **1** (2014). 1

[14] A. Azman, P. S. J. Singh and A. Isahaque, Implications for social work teaching and learning due to the COVID-19 pandemic, *Qualitative Social Work* **20**(1–2) (2021), 553–560. 1

[15] R. P. Finger et al., Lifetime outcomes of anti-VEGF treatment for neovascular AMD, *JAMA Ophthalmology* **138**(12) (2020), 1234–1240. 1

[16] E. M. Azman, N. Yusof, A. Chatzifragkou and D. Charalampopoulos, Stability enhancement of anthocyanins through intermolecular copigmentation, *Molecules* **27**(17) (2022), 5489. 1, 3.11

[17] P. D. Watmough, Reproduction numbers and sub-threshold endemic equilibria, *Mathematical Biosciences* **180** (2023), 29–48. 1, 3.8, 3.11

[18] A. Butt et al., Optimally analyzed fractional coronavirus model with Atangana–Baleanu derivative, *Results in Physics* **53** (2023), 106929. 1, 3.6

[19] K. W. Brhane et al., Mathematical modeling of cholera dynamics with intrinsic growth under constant interventions, *Scientific Reports* **14**(1) (2024), 4616. 1

[20] C. Campos, C. J. Silva and D. F. M. Torres, Numerical optimal control of HIV transmission in Octave/MATLAB, *Mathematical and Computational Applications* **25**(1) (2019), 1. 1, 3.8, 3.11

[21] C. T. Codeço, Endemic and epidemic dynamics of cholera: the role of the aquatic reservoir, *BMC Infectious Diseases* **1**(1) (2001), 1–14. 1

[22] B. S. Castillo-Chavez, Dynamical models of tuberculosis and their applications, *Mathematical Biosciences and Engineering* **1**(2) (2004), 361–404.

[23] W. H. Fleming and R. W. Rishel, *Deterministic and Stochastic Optimal Control*, Springer, (2012). 3.11, 4.2

[24] W. A. Iddrisu, I. Iddrisu and A. K. Iddrisu, Modeling cholera epidemiology using stochastic differential equations, *Journal of Applied Mathematics* **2023**(1) (2023), 7232395.

[25] T. D. Keno, O. D. Makinde and L. L. Obsu, Impact of temperature variability on an SIRS malaria model, *Journal of Biological Systems* **29**(3) (2021), 773–798.

[26] J. Carr, *Applications of centre manifold theory*, Springer Science & Business Media, (2012). 4.1

[27] K. Zhao, Qualitative analysis of a two-group SVIR epidemic model with random effect, *Advances in Difference Equations* **2021**(1) (2021), 1–21.

[28] C. Mary and N. S. Swai, Optimal control of two-strain pneumonia transmission dynamics, *Journal of Applied Mathematics* **2021** (2021), 8835918. 3.11

[29] S. Nana-Kyere et al., Global analysis and optimal control model of COVID-19, *Computational and Mathematical Methods in Medicine* **2022**(1) (2022), 9491847. 3.11

[30] M. M. Ojo and E. F. D. Goufo, Impact of COVID-19 on a malaria-dominated region, *Alexandria Engineering Journal* **65** (2021), 23–39.

[31] Y. Song, P. Liu and A. Din, Analysis of a stochastic epidemic model for cholera with standard incidence rate, *AIMS Mathematics* **8**(8) (2023), 18251–18277. 4.2, 2

[32] S. W. Teklu et al., Analysis of HBV and COVID-19 coinfection model with intervention strategies, *Computational and Mathematical Methods in Medicine* **2023**(1) (2023), 6908757.

[33] I. Zupan, V. Sunde, Z. Ban and B. Novoselnik, Energy flow control algorithm for regenerative braking using Pontryagin's principle, *Energies* **16**(21) (2023), 7346.

[34] M. O. Adewole et al., Extinction of cholera using deterministic and stochastic models incorporating vigilant human compartment, *TWMS Journal of Applied and Engineering Mathematics* **13**(3) (2023), 1222.

[35] M. Ahmed, M. H. O. Khan and M. M. A. Sarker, COVID-19 SIR model: Bifurcation analysis and optimal control, *Results in Control and Optimization* **12** (2023), 100246.

[36] M. B. Alijanzadeh, A. Babayeemehr, K. Rohani, S. Mehrabani and F. Aghajanpour, Role of the World Health Organization in Management of Gastrointestinal Diseases Caused by Contaminated Water in Children in the Middle East: A Review Article, *Journal of Pediatrics Review* **11**(1) (2023), 59–66.

[37] P. Balasubramaniam, M. Prakash, A. F. Rihan and S. Lakshmanan, Hopf bifurcation and stability of periodic solutions for delay differential model of HIV infection of CD4+ T-cells (2014), *Abstract and Applied Analysis* **2024**(1) (2024), 838396. 3.1, 4.1

[38] J. P. Romero-Leiton, Optimal control problem for cholera and cost-effectiveness analysis, *Journal of Mathematical & Fundamental Sciences* **53**(2) (2021).

[39] P. D. Watmough, Reproduction numbers and endemic equilibria, *Mathematical Biosciences* **180** (2002), 29–48.

[40] H. O. Namawejje, Optimal control of cholera under vaccination and treatment interventions, *Journal of Mathematics Research* **10**(5) (2018), 137–152.

[41] L. S. Pontryagin, *The Mathematical Theory of Optimal Processes*, Wiley, (1986).

[42] H. L.-L. Shaikh, Current and future cholera vaccines, *Vaccine* **38** (2020), A118–A126.

[43] P. V. Driessche and J. Watmough, Reproduction numbers and sub-threshold endemic equilibria for compartmental models of disease transmission, *Mathematical biosciences* **180**(1-2) (2002), 29–48.

[44] A. S. Yakubu and K. S. Shammah, Sensitivity analysis of tuberculosis model with control measure, *African Journal of Mathematics and Statistics Studies* **6**(3) (2023), 17–34.

[45] X. Han and P. E. Kloeden, *Random Ordinary Differential Equations*, Springer, (2017).

[46] A. Ouakka, A. Alla Hamou and A. El Azzouzi, A mathematical model for epidemic dynamics with multiple vaccines, *Nonlinear Dynamics* **113** (2025), 23753–23783.

[47] A. Alla Hamou, E. Azroul and S. L'kima, Fractional-order modeling of parasite-produced marine diseases, *Modeling Earth Systems and Environment* **10**(5) (2024), 6357–6372.

[48] A. Alla Hamou, E. Azroul and S. L'kima, The effect of migration on the transmission of HIV/AIDS using a fractional model: Local and global dynamics and numerical simulations, *Mathematical Methods in the Applied Sciences* **47**(8) (2024), 6868–6891.

[49] A. Alla Hamou, E. Azroul, S. Bouda and M. Guedda, Mathematical modeling of HIV transmission in a heterosexual population: incorporating memory conservation, *Modeling Earth Systems and Environment* **10**(1) (2024), 393–416.

[50] Z. Hammouch, M. O. Jamil, A. Alla Hamou and C. Unlu, Dynamics investigation and numerical simulation of fractional-order predator-prey model with Holling type II functional response *Discrete and Continuous Dynamical Systems-S* **18**(5) (2025), 1230–1266.

[51] S. I. Ouaziz, A. A. Hamou and M. El Khomssi, Dynamics and optimal control strategies of corruption model, *Results in Nonlinear Analysis* **5**(4) (2022), 423–451.

[52] M. Zamir, F. Nadeem, T. Abdeljawad and Z. Hammouch, Threshold condition and non pharmaceutical interventions's control strategies for elimination of COVID-19, *Results in Physics* **20** (2021), 103698.